# Supporting Information

***Title:*** **Dextran Vesicular Carriers for Dual Encapsulation of Hydrophilic and Hydrophobic Molecules and Delivery into Cells**

***Authors:*** P. S. Pramod, Kathryn Takamura, Sonali Chaphekar,

Nagaraj Balasubramanian and M. Jayakannan

**Contents** **Page no.**


| | |
|---|---|
| GPC, NMR and FTIR spectra of DEX-PDP and DEX-CAR | 2-9 |
| DLS of DEX-PDP-10 and DEX-PDP-19 | 10 |
| FE SEM ,AFM image and SLS data of DEX-PDP-5 | 11-14 |
| DLS and TEM image of DEX-SA-7, DEX-PDP-10 and DEX-CAR-10 | 15-17 |
| Single crystal data and Packing of of PDP-acid | 18-20 |
| DSC thermograms of CAR acid, PDP acid and SA | 21 |
| pH dependent DLS data and CVC calculation | 22-23 |
| Dialysis photographs, Fluorescent micrographs of Rh-B | 24-25 |
| AFM and SLS data of DEX-PDP-CPT | 26 |
| AFM and SLS data of DEX-PDP-Rh-B | 27 |
| HPLC data | 28-30 |
| HRMS spectra of PDP-acid cleaved from DEX-PDP | 31 |
| Rh-B *in-vitro* release with 30 U esterase | 32 |
| Flourescent micrographs of DEX-PDP-CPT and cell line data | 33-34 |
| TGA profile of DEX-PDP | 35 |
| NMR data of PDP and CAR ester, acid and DEX-SA | 36-40 |

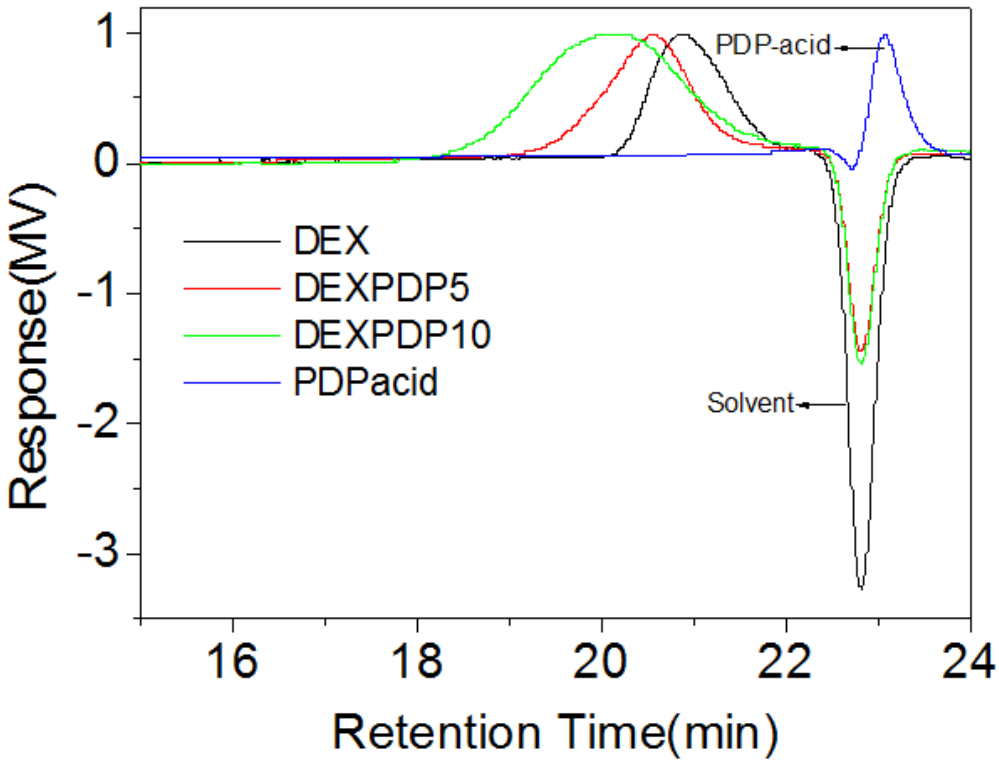


**Figure SF1.** *GPC Chromatograms of dextran, DEX-PDP-5,DEX-PDP-10 and PDP-acid in dimethyl formamide at 25 ℃.*

Note: GPC chromatogram of the modified dextran and starting materials were recorded to check the purity of the newly synthesized polymer scaffold. Mono-model distribution of modified dextran confirmed the high purity of the samples. The shift in the chromatogram of DEX-PDP-5 and DEX-PDP-10 in the low retention time compared to dextran further validate the substitution of PDP-acid on the dextran backbone.

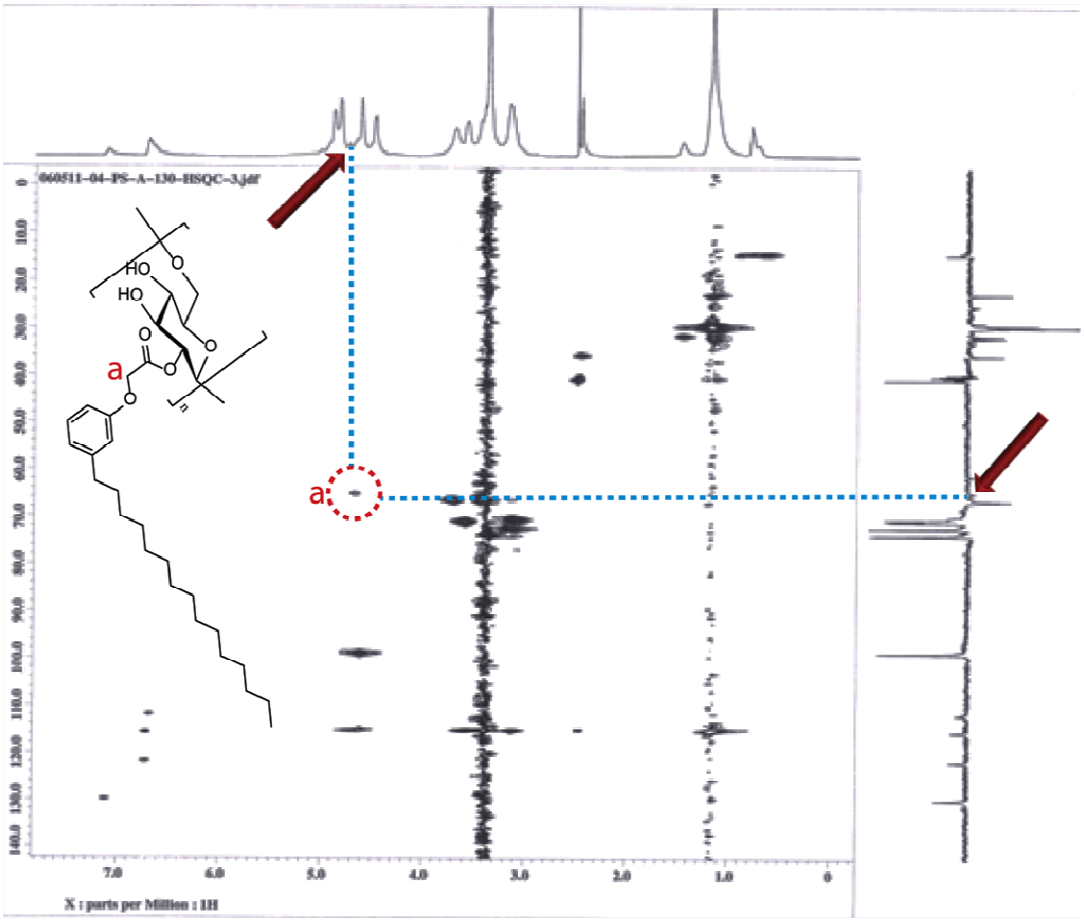


**Figure SF2.** *2-D NMR-HSQC spectrum of DEX-PDP in DMSO (d6)*

Note: 2-D NMR-HSQC spectrum was recorded to confirm the structure of DEX-PDP. The contour marked as "**a**" in the spectrum corresponds to Ar-O-**$\underline{CH_2}$**-COO-dex, substantiated the linkage between hydrophilic dextran and hydrophobic PDP-acid.

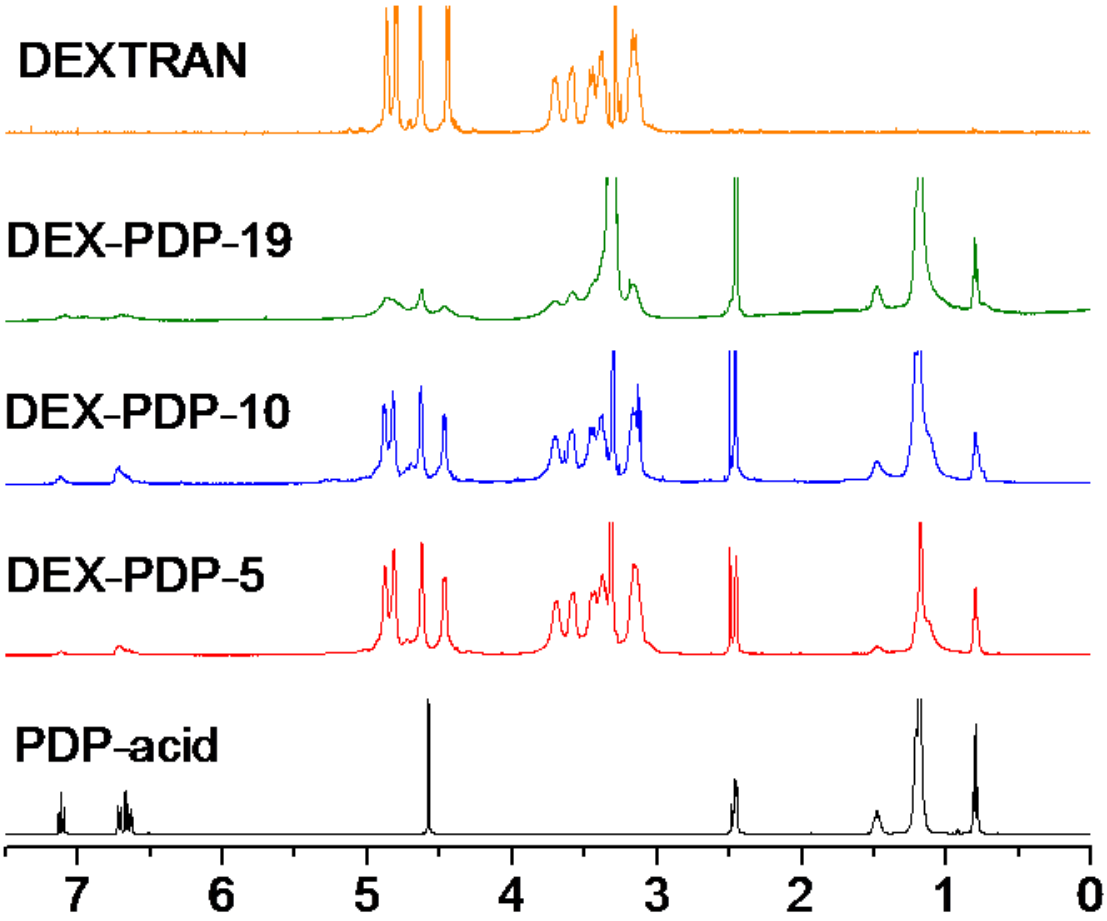


**Figure SF3.** *Stack plot of PDP-acid DEX-PDP-5, DEX-PDP-10 and DEX-PDP-19 and Dextran NMR in DMSO (d6).*

Note: The degree of substitution of hydrophobic unit on dextran back bone was calculated by comparing the peak intensities of the anomeric protons in dextran at 4.62 ppm and PDP aromatic protons at 7.2 ppm.

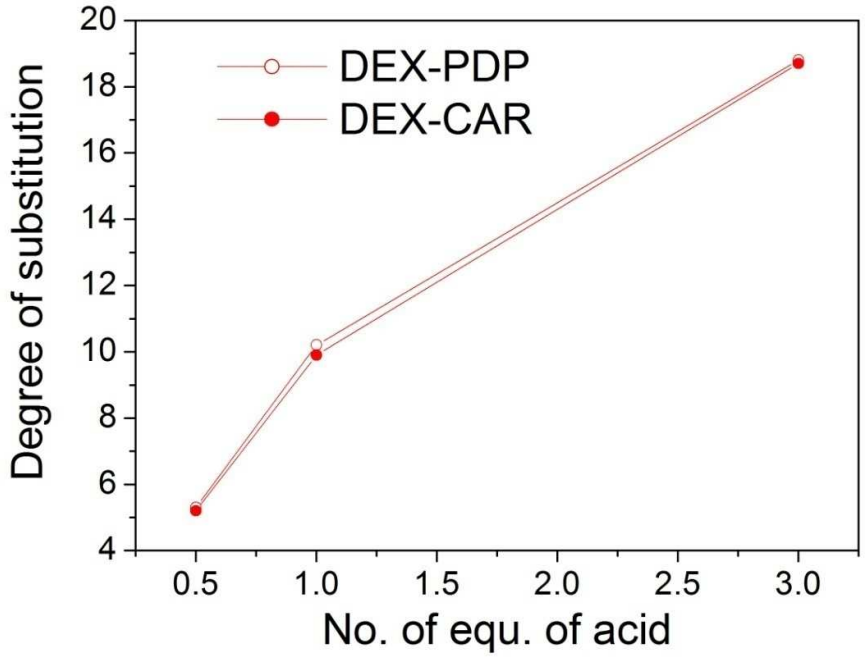


**Figure SF4.** *Plot of degree of substitution on dextran backbone versus no.of equivalents of PDP-acid in the feed.*

Note: Plot of degree of substitution (DS) versus no.of equivalents of acid in the feed indicated that the substitution of hydrophobic units increased in a linear fashion with increase in the amount of acid. This confirms that polymer scaffold with adjustable DS value can be synthesized by changing the amount hydrophobic unit in the feed.

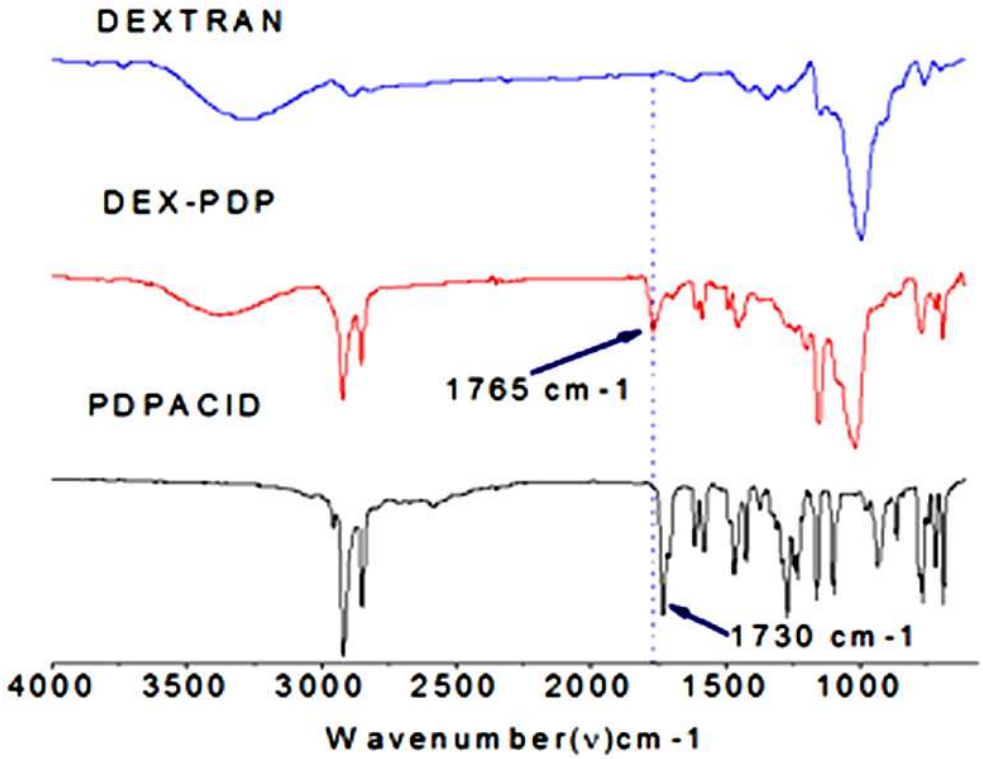


**Figure SF5.** *FTIR spectra of Dextran, DEX-PDP and PDP-acid.*

Note: FT-IR spectrum of PDP-acid displayed a discrete stretching band at 1730 $cm^{-1}$ with respect to -C=O stretching frequency of carboxylic acid functional group. But in the case of DEX-PDP, where dextran and PDP-units were linked through ester linkage, spectrum showed a distinct peak at 1765 $cm^{-1}$. This peak corresponds to the ester –C=O group supported the structure of the scaffold. Dextran alone is devoid of any peak in this region.

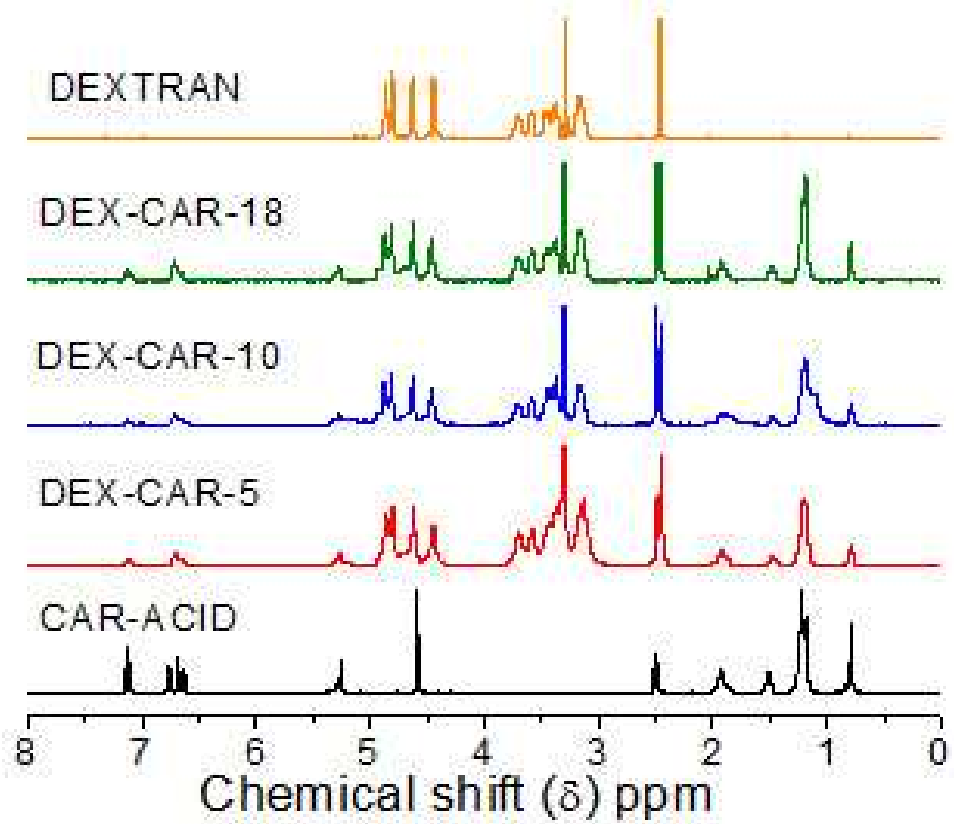


**Figure SF6.** *Stack plot of CAR-acid , DEX-CAR-5, DEX-CAR-10, DEX-CAR-18 and Dextran NMR in DMSO (d6).*

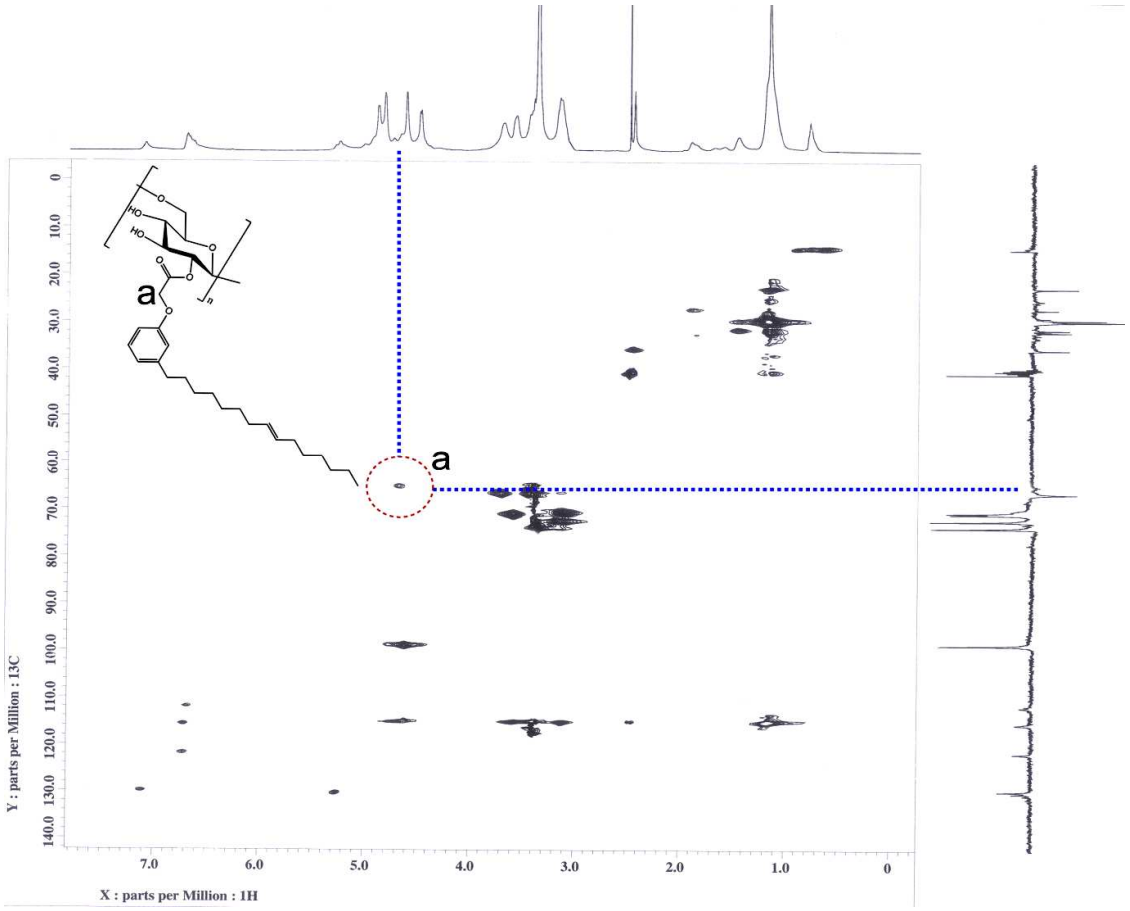


**Figure SF7.** *2-D NMR-HSQC spectrum of DEX-CAR in DMSO (d6)*

*Note:* The contour marked as "a" in the spectrum corresponds to Ar-O-**$\underline{CH_2}$**-COO-dex confirms the structure of DEX-CAR.

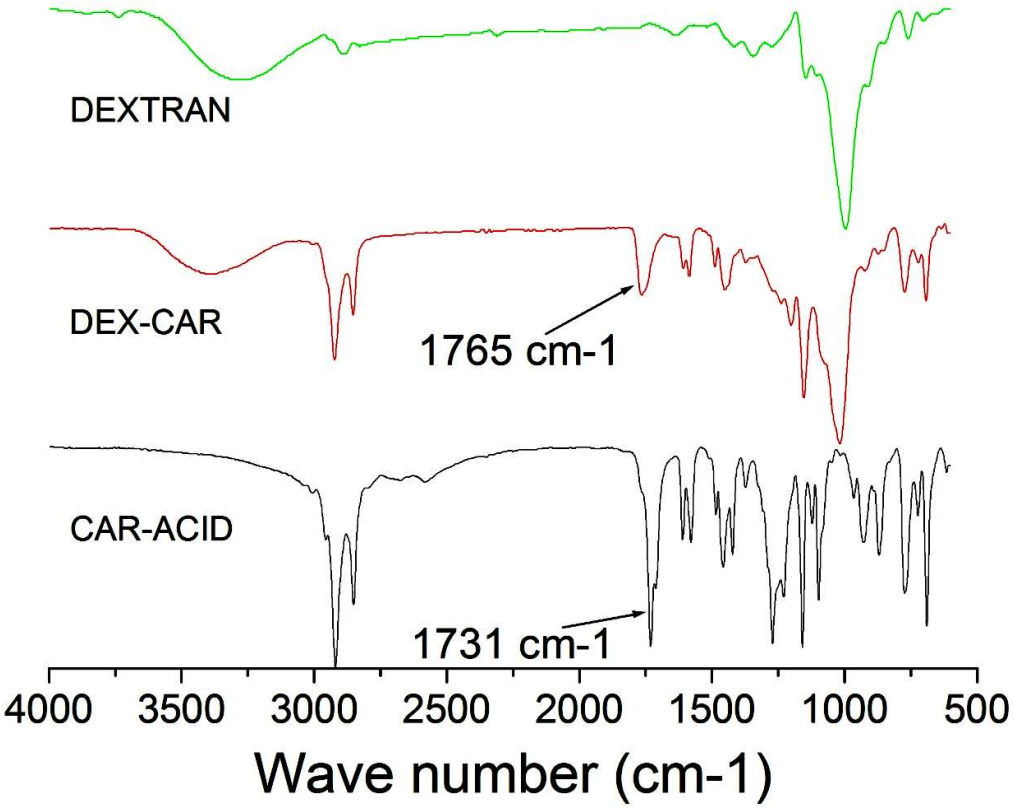


**Figure SF8.** *FTIR spectra of Dextran, DEX-CAR and CAR-acid.*

Note: The -C=O stretching frequency of carboxylic acid functional group in CAR acid was appeared at 1731 $cm^{-1}$. But DEX-CAR spectrum showed a distinct peak at 1765 $cm^{-1}$ as observed in DEX-PDP. This peak corresponds to the ester –C=O group. This supports the structure of DEX-CAR.

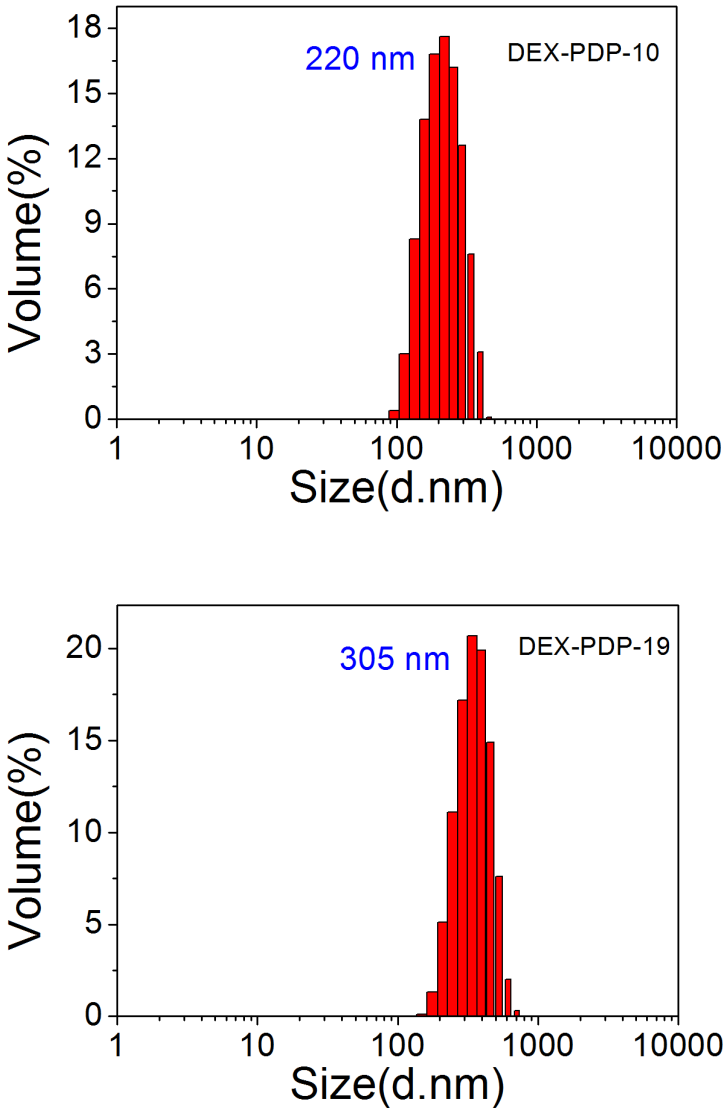


**Figure SF9.** *DLS histograms of DEX-PDP-10 and DEX-PDP-19*

Note: DLS histograms in PBS (pH 7.4) reveal the mono-model distribution pattern of DEX-PDP-10 and DEX-PDP19 with an average size of 220 nm and 305 nm respectively.

(a)

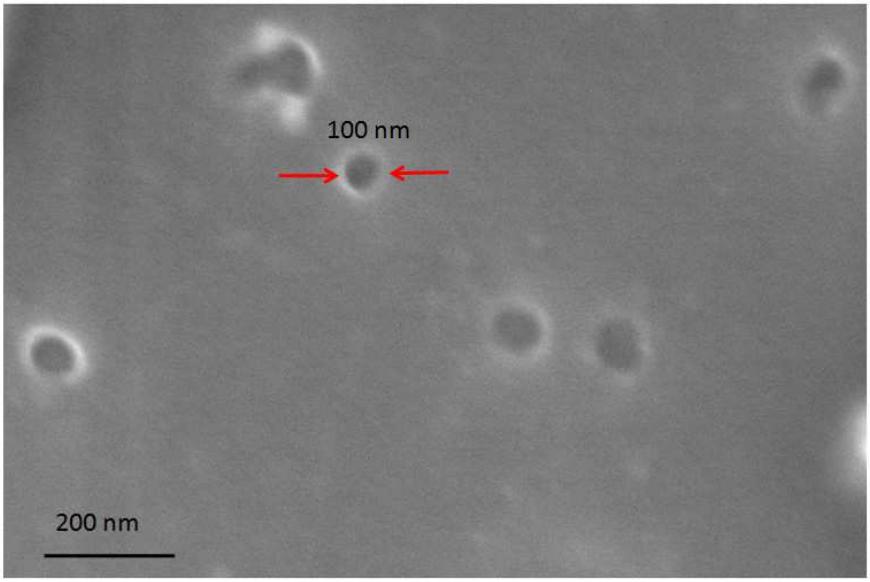


(b)

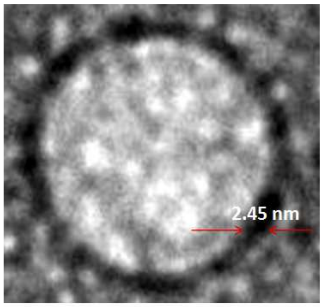


**Figure SF10.a.** *FESEM micrograph of DEX-PDP-5.* ***b****. Magnified TEM image of DEX-PDP-5 vesicle.*

Note: **a**. SEM micrograph of DEX-PDP-5 clearly indicates that the polymer scaffold forms spherical vesicular aggregate. A magnified view of this aggregate is shown in the inset figure. **b**. An enlarged view of TEM image of vesicle formed from DEX-PDP-5 visibly shows the hollowness inside and a hydrophobic membrane with thickness measured as 2.45 nm.

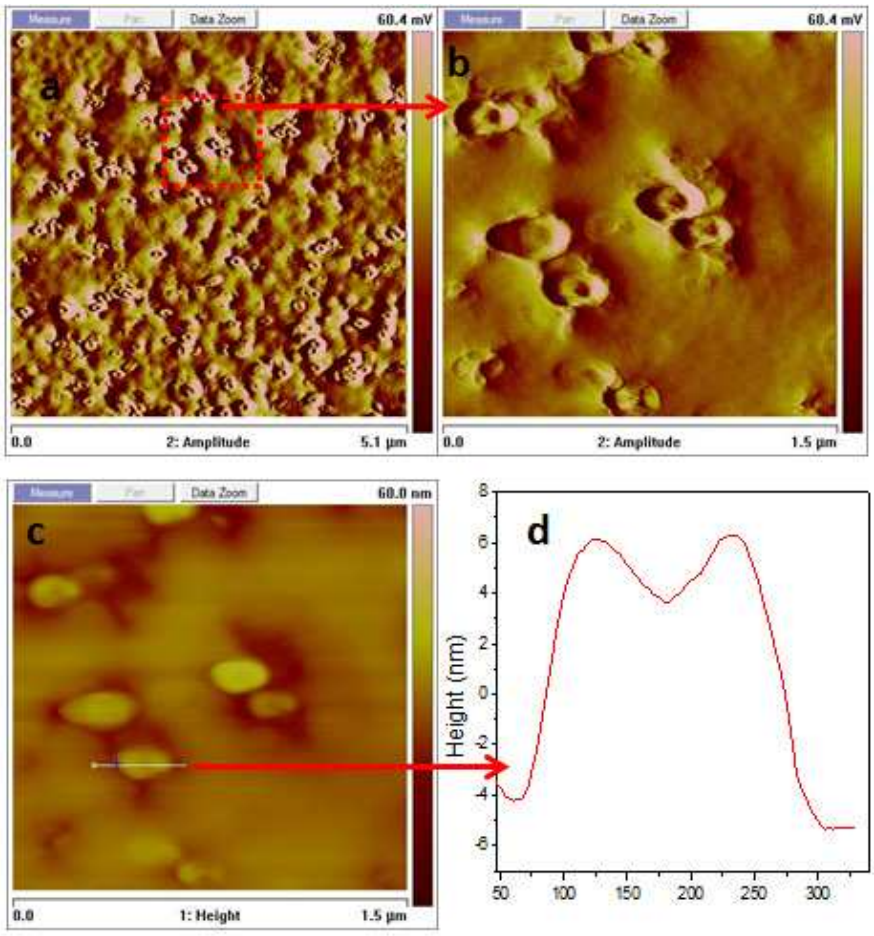


**Figure SF11.** *AFM micrographs of DEX-PDP-5: phase image (a), Magnified view (b) Height image (c) and Height profile (d)*

Note: The surface difference in the vesicular self assembly dissipates different responses to the force of AFM tip. As a result, the phase image of DEX-PDP was observed as high periphery (harder surface) and lower center (Soft interior). While relatively smooth surface was observed in height image. A similar pattern was seen in the height profile.

(a)

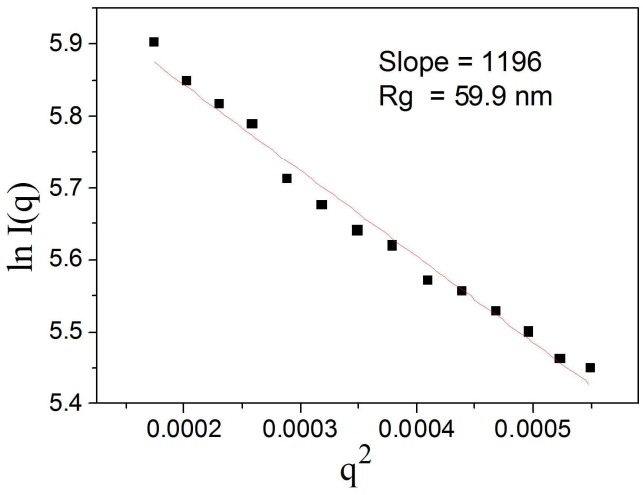


(b)

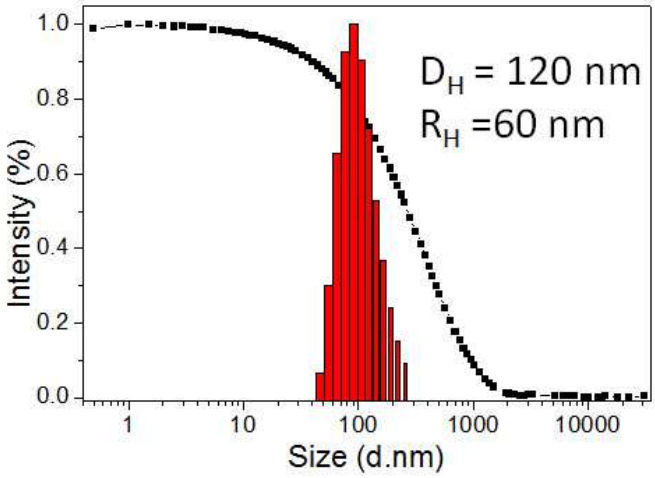


**Figure SF12.** Guinier plot (from SLS experiment) and DLS histogram of DEX-PDP-5

Note: In Static Light Scattering experiment Intensity was measured as a function of q (which was varied by angle $\theta$. The variable $q$ represents the scattering vector magnitude. It is given by the equation:

$$q = \frac{4\pi n \sin(\theta/2)}{\lambda_o}$$

Here n is the solution refractive index and $\lambda_o$ is the incident wavelength, ie: 632.8 nm. The radius of gyration (Rg) was calculated from Guinier plot, given by:

$$\ln(I(q)) = \ln(I(0)) - \frac{q^2 R_g^2}{3}$$

Here slope of the graph is $R_g{}^2/3$ . In the case of DEX-PDP-5, Slope = 1196. So $R_g$= 59.9 nm

The hydrodynamic radius ($R_h$)of DEX-PDP-5 was obtained from DLS as 60 nm. Using this value the ratio $R_g/R_h$was calculated as 1. This clearly pointed the vesicular structure of DEX-PDP-5.

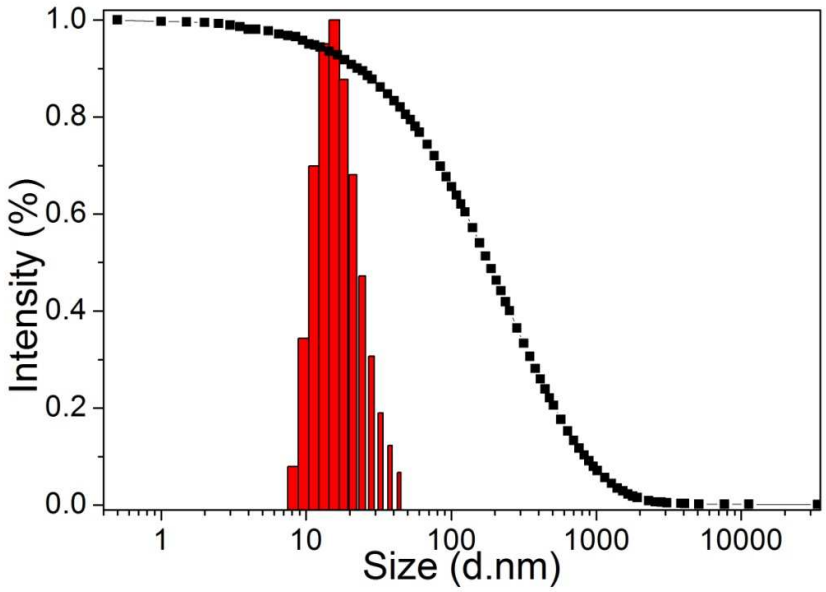


**Figure SF13.** *DLS histograms of DEX-SA-7*

Note: DLS histograms in PBS (pH 7.4) reveal the mono-model distribution pattern of DEX-SA-7 with an average size of 25 nm

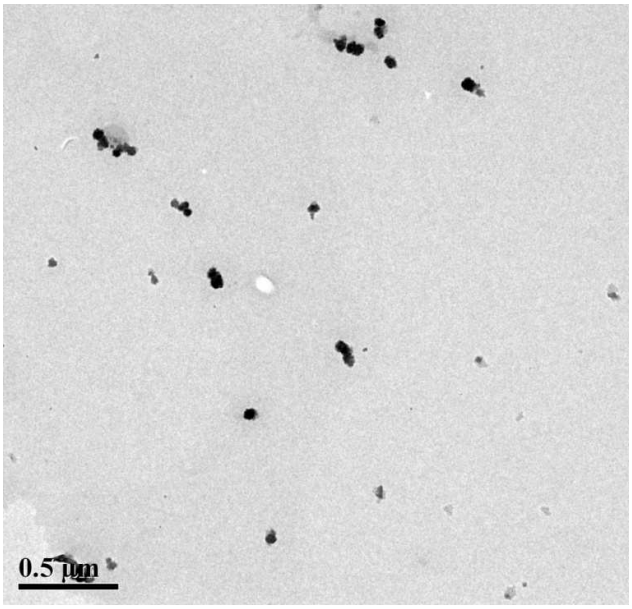


**Figure SF14.** *HR-TEM image of DEX-SA-7*

Note: Typically, HR-TEM image of the nanoparticles are appeared as solid dark particles, due to the change in phase and amplitude of electron wave interacting with the nano materials. Here stearic acid modified dextran was seen as solid spherical nanoparticles (as observed by Du *et al, ACS Nano* **2010**, *4*, 6894.) rather than hollow vesicular structure noticed in DEX-PDP-5 (see figure 3b and 3d in the main text). This observation is pointing towards the importance of the hydrophobic unit in the self assembly process of polysaccharides.

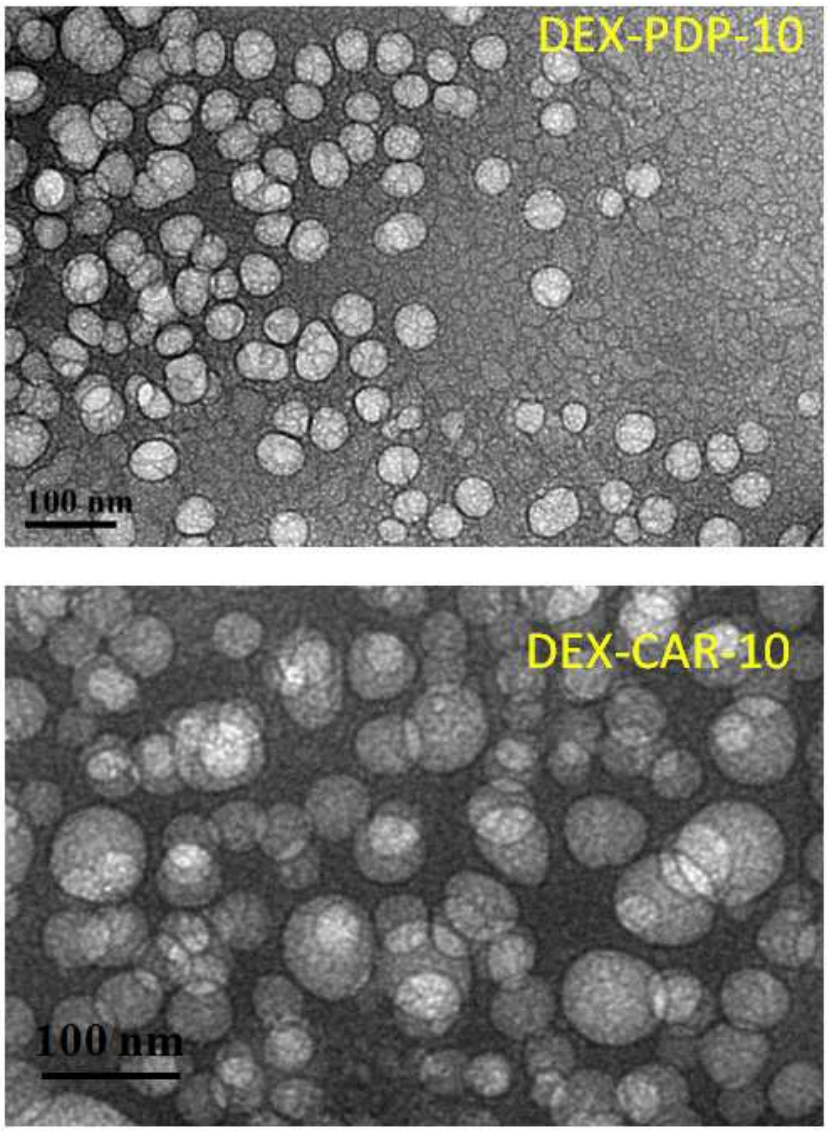


**Figure SF15.** *TEM images of DEX-PDP-10 and DEX-CAR-10*

**Table-ST1:** Unit cell parameters of PDP-Acid molecule

| **Compound** | **PDP-acid** |
|---|---|
| Formula | $C_{23}H_{38}O_3$ |
| recrystn solv | DCM/Acetone |
| mol wt | 362 |
| Colour, habit | Colorless, needle |
| temp(K) | 200 |
| system | Triclinic |
| space group | P-1 |
| a, (Å) | 5.382 |
| b, (Å) | 6.929 |
| c, (Å) | 29.95 |
| α, (deg) | 85.615 |
| β, (deg) | 89.872 |
| γ, (deg) | 73.155 |
| V, $Å^3$ | 1065.6 |
| $d_{cacl}$ ,Mg /$m^3$ | 1.130 |
| μ($mm^{-1}$) | 0.072 |
| GOF | 0.931 |
| Independent reflections | 5127 |
| Reflections collected | 15738 |
| θ range | 1.36 to 28.29 |
| No. of refined parameters | 236 |
| $R_1$ ( on F, I>2σ (I)) | 0.1023 |
| $wR_2$ (on $F^2$, all data) | 0.3119 |

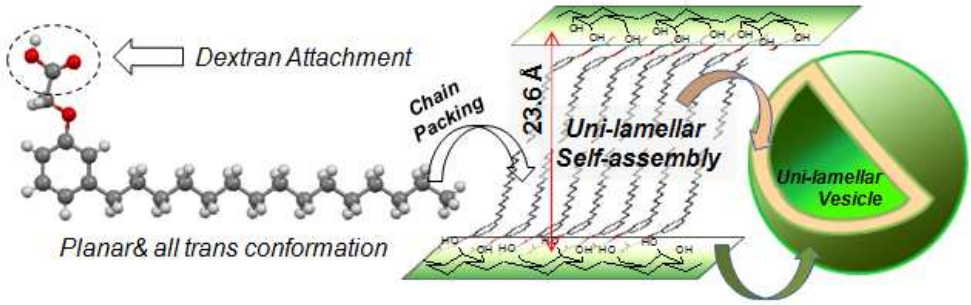


**Figure SF16 a.** Schematic representation of crystal packing of hydrophobic unit in the unilamellar vesicle formation.

Note: This molecule crystallized in triclinic lattice in the space group of P-1 and their unit cell parameters were determined as: a = 5.382 Å, b = 6.929 Å, c = 29.95 Å, α =85.615°, β = 89.872° and γ = 73.155°. PDP-acid was planar and the pentadecyl chains were orientated towards each other to form a hydrophobic layer of thickness 23.6 Å (or 2.36 nm, see figure 3e). The wall thickness of the dextran vesicles (~ 2.45 ± 0.18 nm (n = 50), from TEM images) was almost identical to that of the hydrophobic layer distance (~2.36 nm, from the crystal structure) indicating that the thin hydrophobic walls in the vesicles were constituted by the long tails in the PDP units.

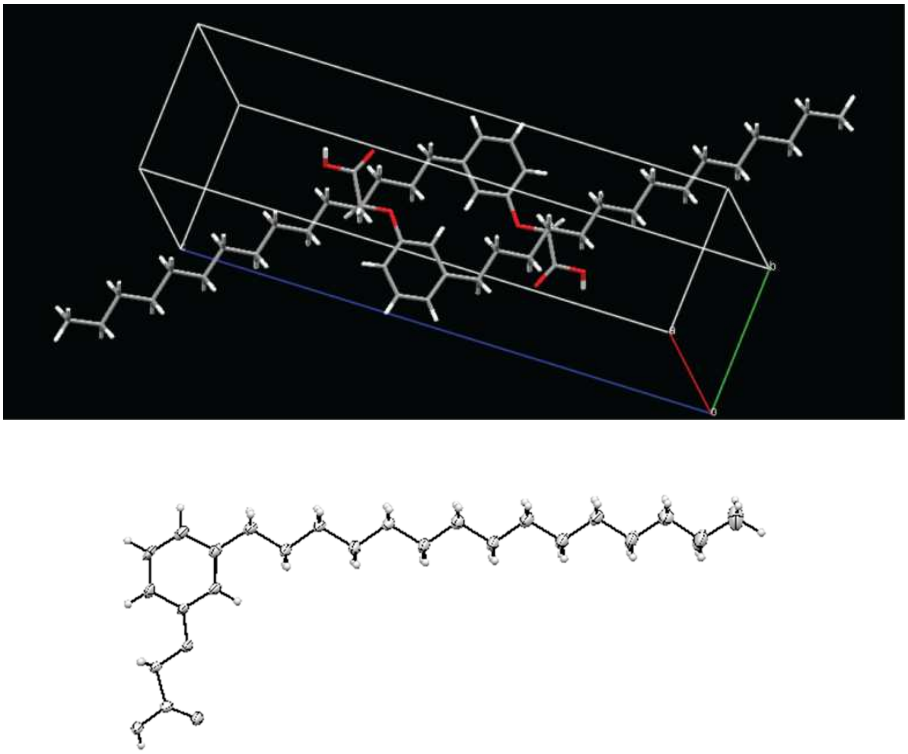

**Figure SF16 b.** Unit cell and ORTEP diagram for the single crystal of compound PDP-acid

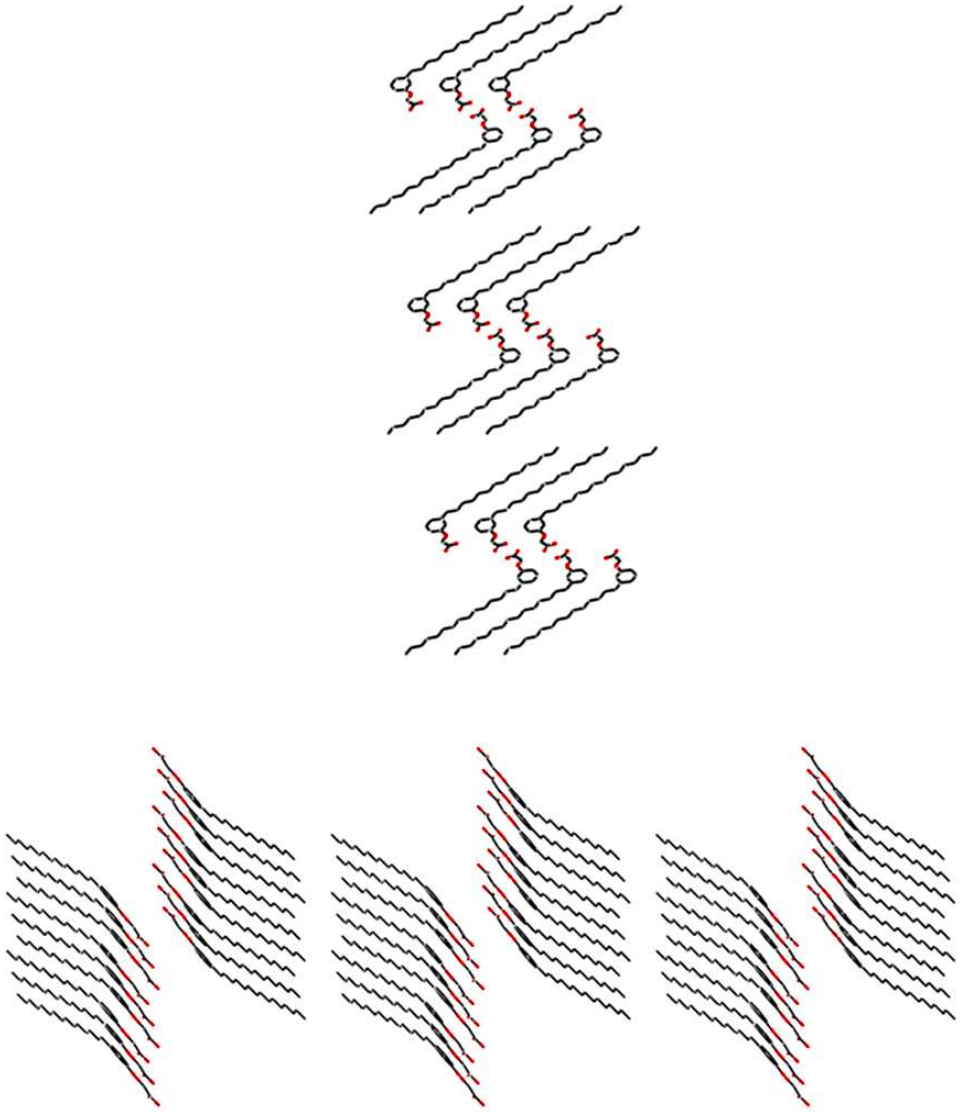

**Figure SF17.** Molecular packing diagram for compound PDP-Acid along a and b* axis respectively

**Note:** Single crystal packing of PDP-acid iilustrate the packing of the alkyl chains, which constitute the hydrophobic layer in the dextran based unilamellar vesicles

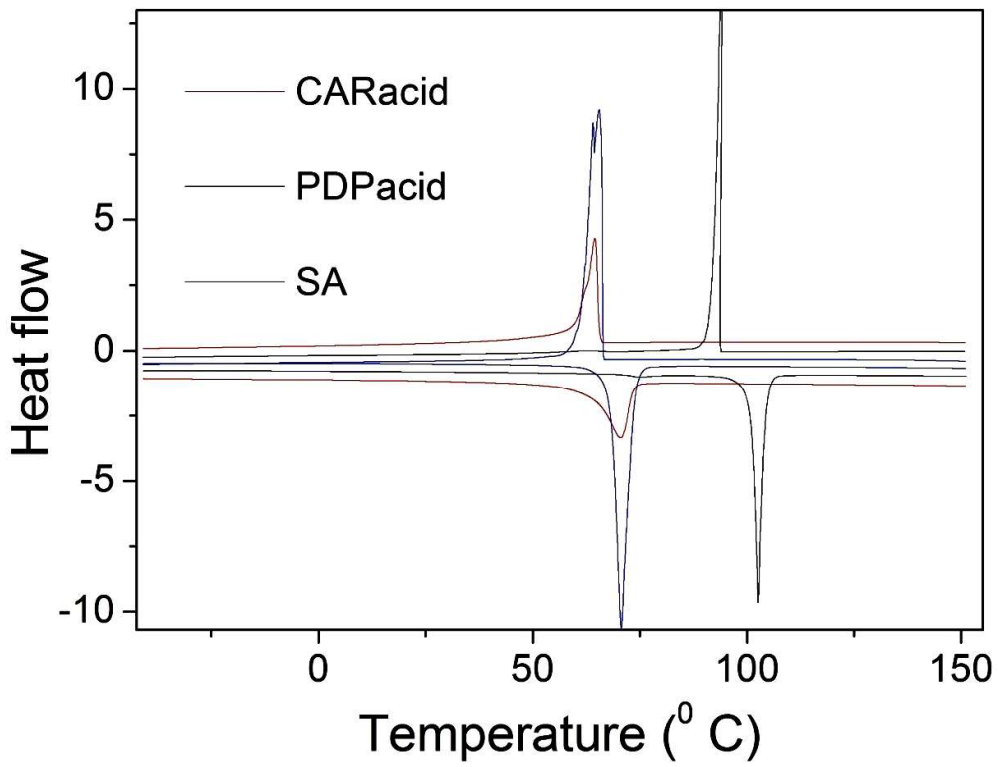


**Figure SF18.** DSC thermograms of CAR acid, PDP acid and SA in the heating and cooling cycle at 10° C /min.

**Table ST2.** Enthalpies of Melting and crystalline transitions of PDP acid, CAR acid and SA

| **Sample** | **Tm** (°C) | **ΔHm** (KJ/mol) | **Tc** (° C) | **ΔHc** (KJ/mol) |
|---|---|---|---|---|
| PDP-acid | 101.54 | 52.8 | 95.28 | 49.5 |
| CAR-acid | 65.48 | 23.3 | 63.94 | 17.9 |
| SA | 68.88 | 54.2 | 65.13 | 47.7 |

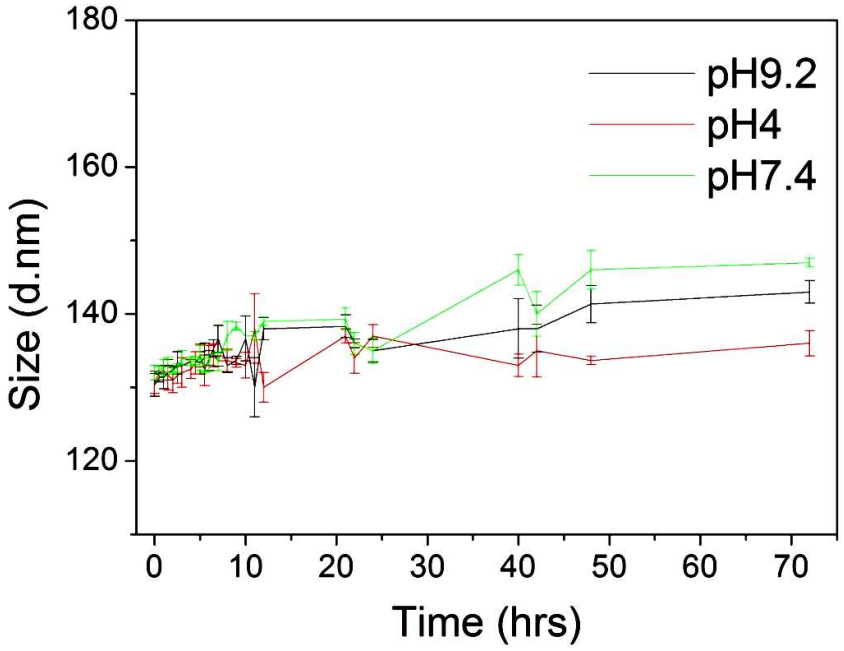


**Figure SF19.** *DLS aggregation size of DEX-PDP-5 at various pH*

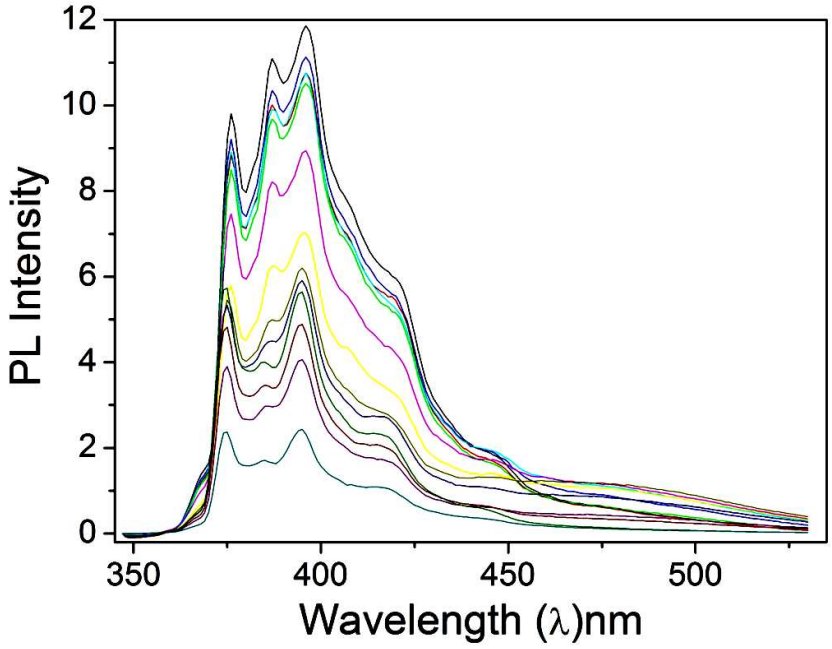


**Figure SF20.** *Emission spectra of pyrene with DEX-PDP-5 at different concentrations of polymer.*

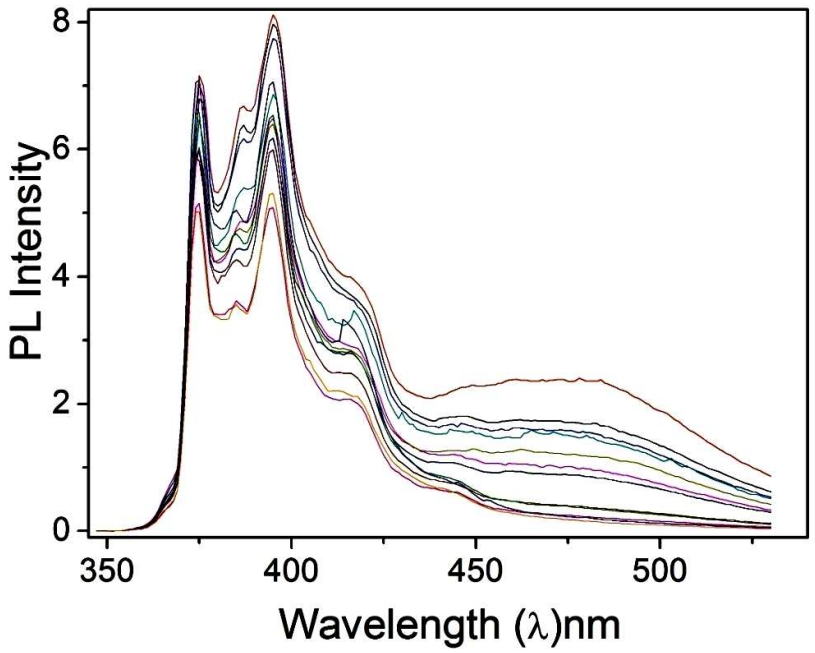


**Figure SF21.** *Emission spectra of pyrene with DEX-CAR-5 at different concentrations of polymer.*

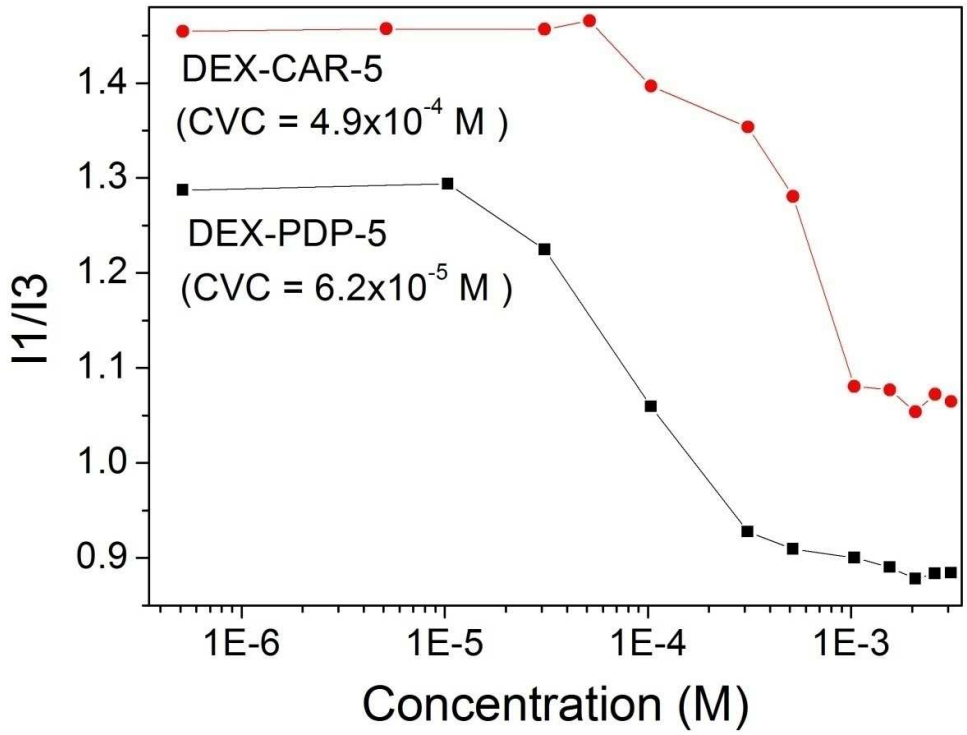


**Figure SF22.** I1/I3 Vs Concentration plot of DEX-PDP-5 and DEX -CAR-5

Note: Critical vesicular concentration of DEX-PD5 and DEX-CAR-5 was determined using pyrene as fluorescent probe. CVCs was calculated as $6.2X10^{-5}$ and $4.9X10^{-4}$ M respectively.

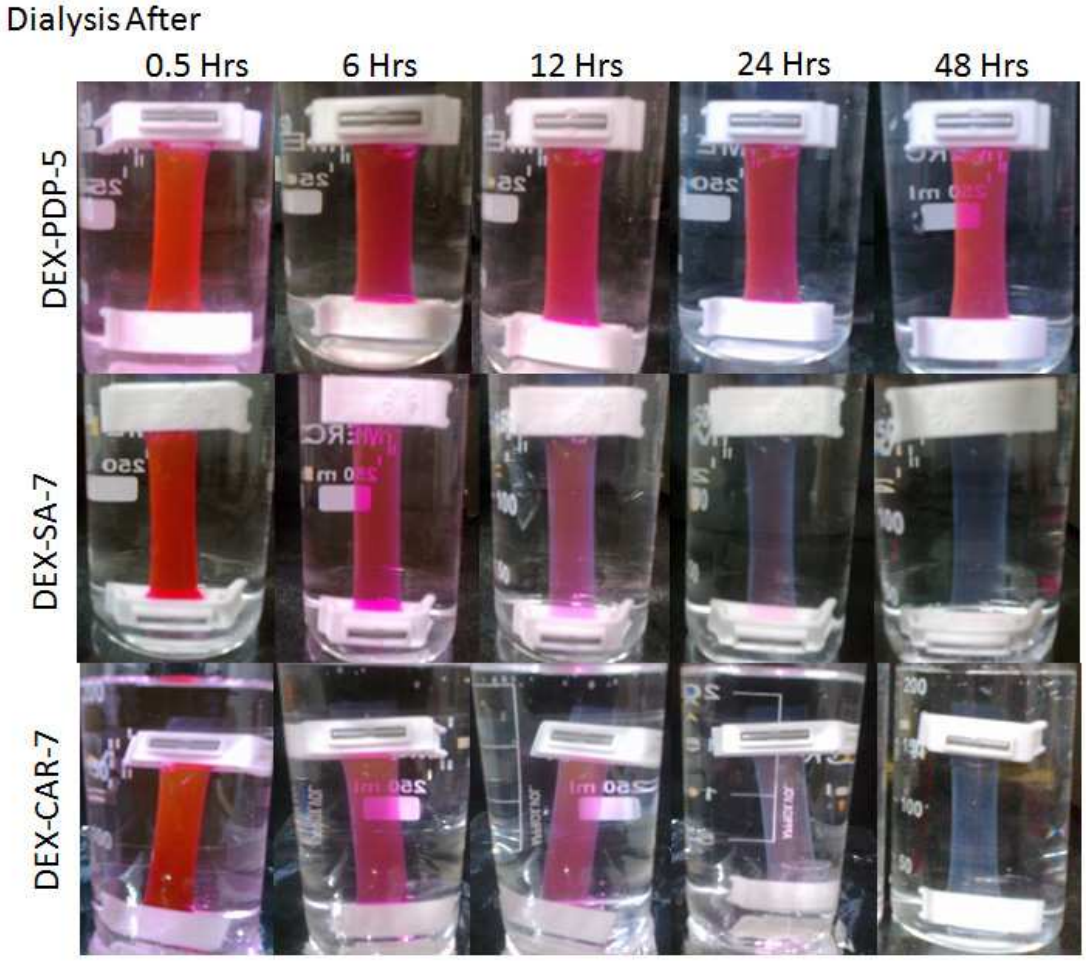


**Figure SF 23.** Dialysis photographs of rhodamine with DEX-PDP-5, DEX-CAR-5 and DEX-SA-7 taken at regular interval of time.

Note: The photographs clearly indicate that the rhodamine is well stabilized in DEX-PDP-5 (It was checked up to 7days, Similar results were observed.) while the dye was almost completely leached out from DEX-CAR-5 and DEX-SA-7 within 48 hrs. This pointed towards stable vesicular structure formed by DEX-PDP-5. The photographs were taken by removing dialysate with fresh water to get better visibility.

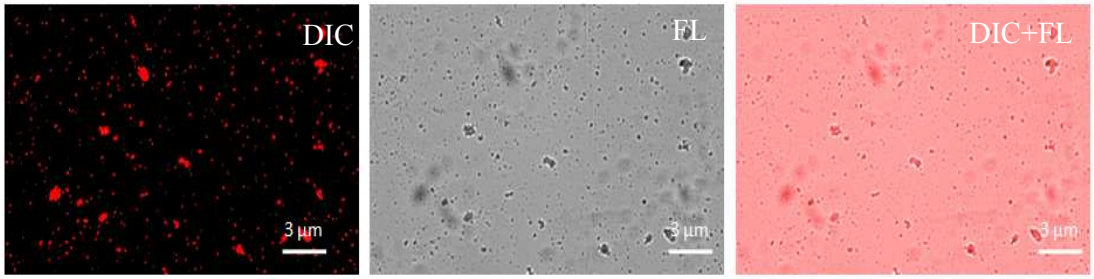


**Figure SF 24:** Fluorescent micrographs of Rh-B encapsulated in DEX-PDP-5

Note: Fluorescent micrographs of encapsulated sample showed spherical vesicular structure with hollow cavity inside. Merging of the images obtained from transmitted mode (DIC) and reflected mode (FL) provided direct evidence for the rhodamine encapsulation

(a)

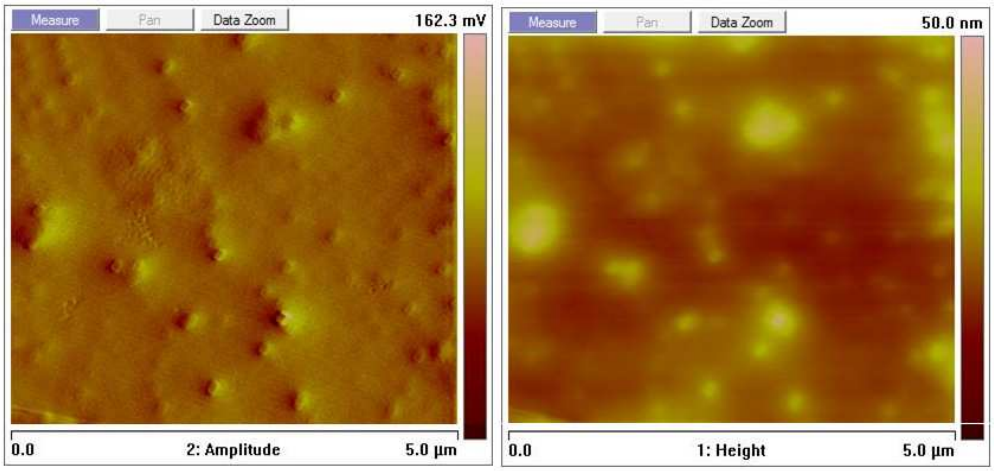


(b) (c)

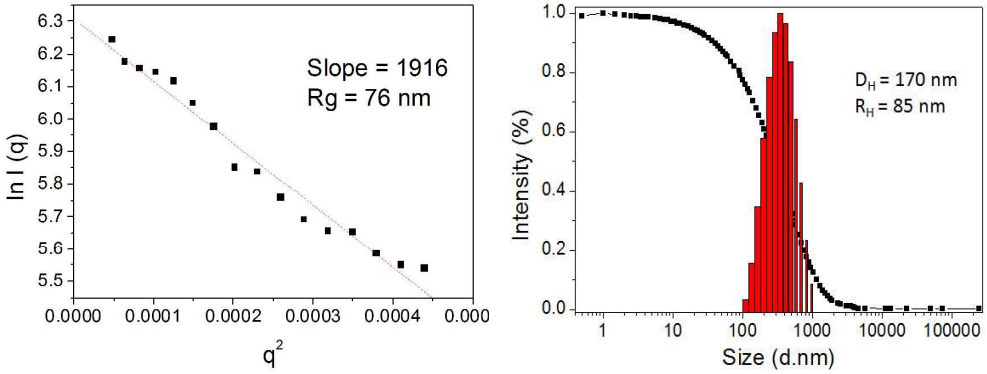


**Figure SF 25:** Phase and Height image of DEX-PDP-Rh-B (a) Guinier plot of DEX-PDP-Rh-B from SLS experiment (b) and DLS histogram of DEX-PDP-Rh-B (c)

**Note:** The AFM image of the loaded vesicle further proves the morphology of the DEX-PDP-Rh-B. The static light scattering (SLS) experiment was performed in the similar way as done for DEX-PDP-5. The $R_g$/ $R_H$ ratio was calculated as 1.11, where radius of gyration $R_g$ = 76 nm (from SLS) and hydrodynamic radius $R_H$ = 85 nm (from DLS), further corroborate vesicular structure

(a)

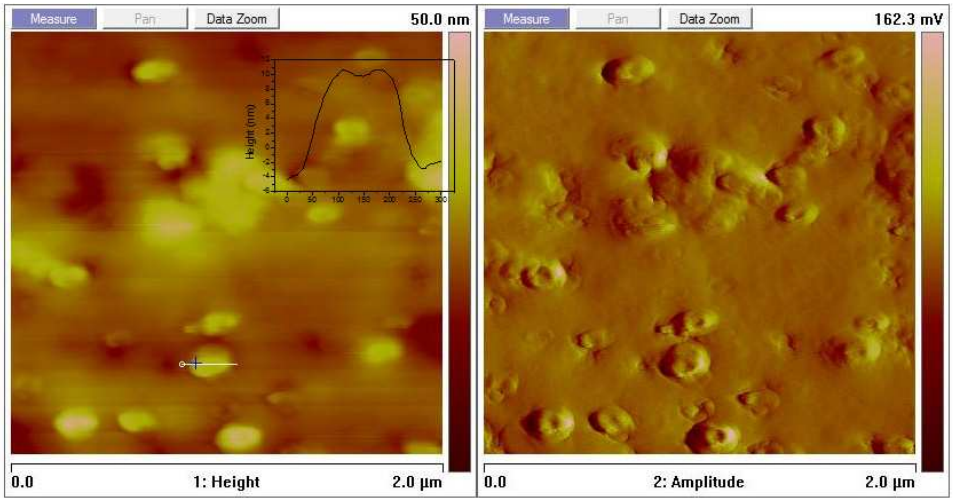


(b) (c)

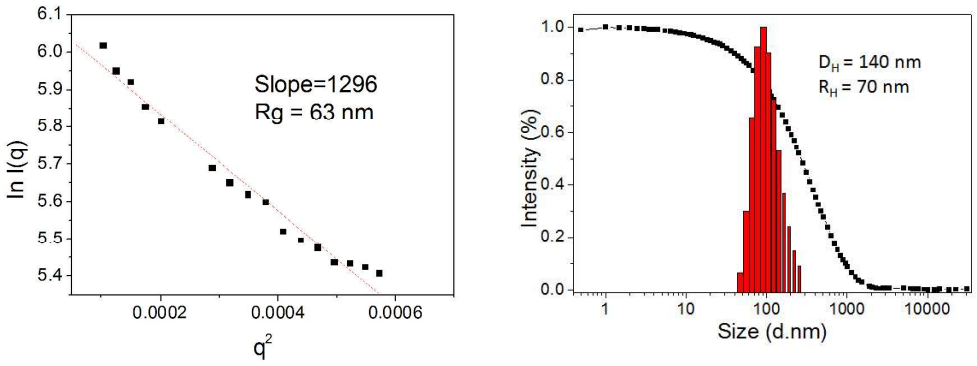


**Figure SF26.** Height and phase image of DEX-PDP-CPT(a) Guinier plot of DEX-PDP-CPT from SLS experiment(b) and DLS histogram of DEX-PDP-CPT (c)

Note: The AFM micrograph of DEX-PDP-CPT also confirms the vesicular nature of the aggregates. The diameter and the height of the aggregates were calculated as 140 nm and 10 nm, respectively. The static light scattering experiment was carried out as described for DEX-PDP-5 and the ratio of $R_g/R_H$ was determines as 1.11, where $R_g$ = 63 nm (from SLS) and $R_H$ = 70 nm (from DLS).

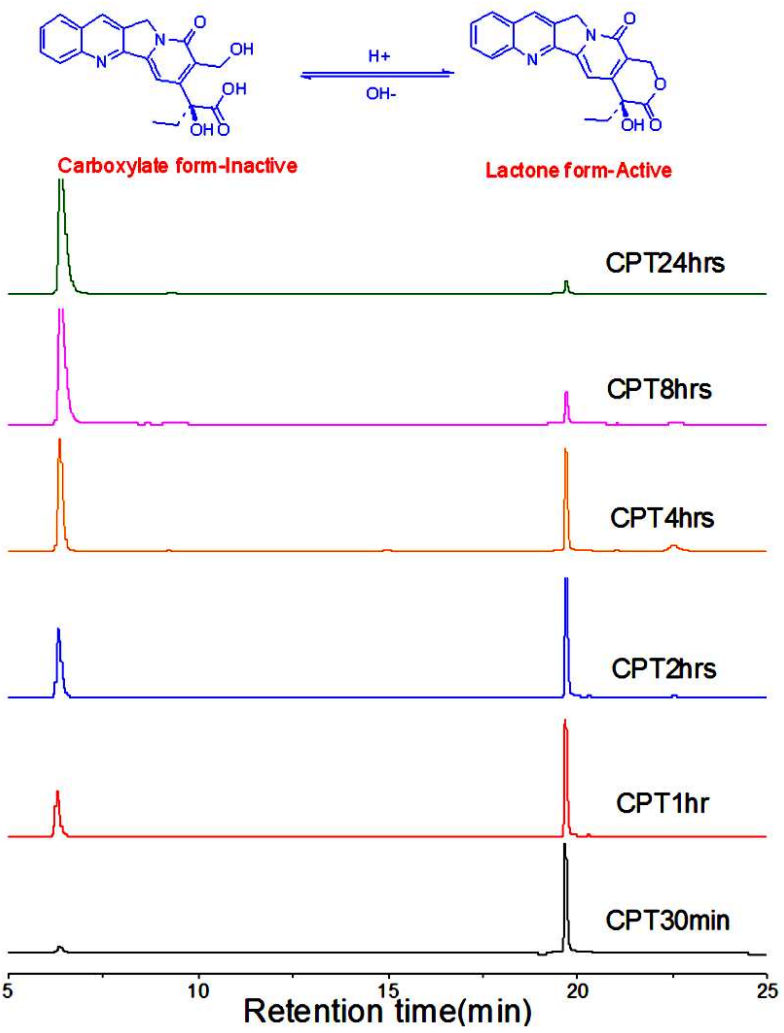


**Figure SF27.** *HPLC traces of CPT incubated in PBS pH 7.4 at different time intervals*

Note: CPT was incubated with PBS (pH 7.4) buffer. It was subjected to high performance LC analysis using acetonitrile: TEAA buffer as mobile phase at different time intervals. The lactone and carboxylate form of the CPT could able to separate in single chromatographic run with a retention time of 19.2 min and 7.2 min, respectively. HPLC traces showed that free CPT undergoes rapid hydrolysis from lactone to carboxylate form at physiological pH leading to only 4 % of active form after 24 h of incubation.

(a)

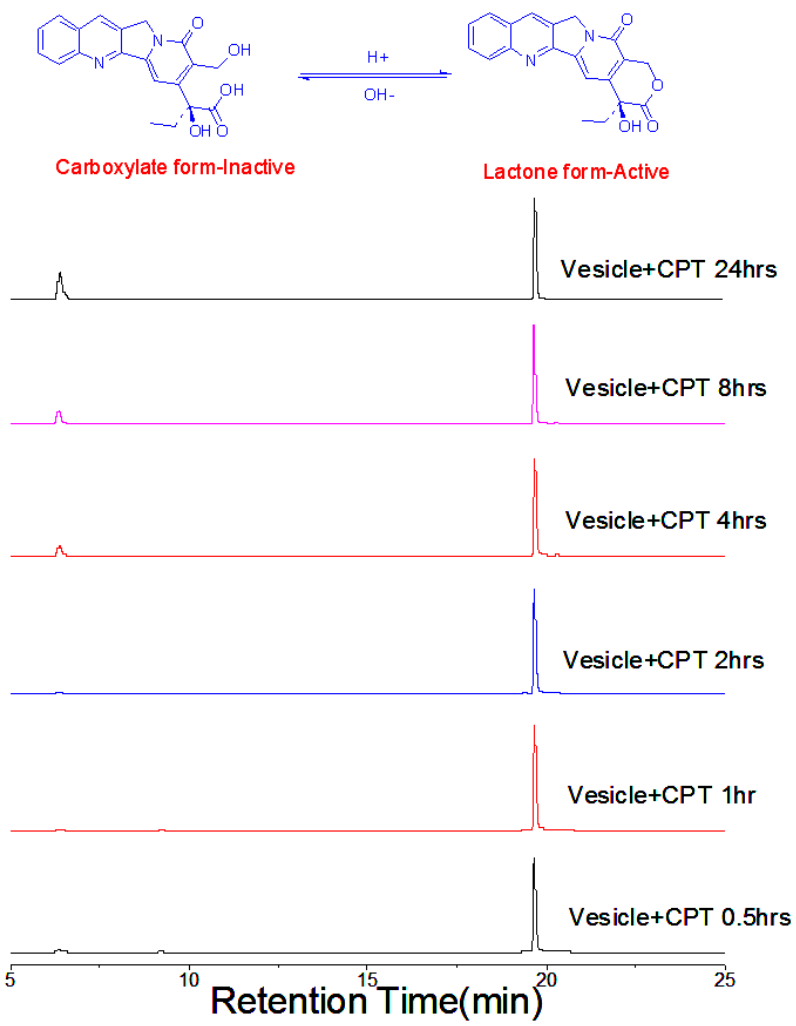


(b)

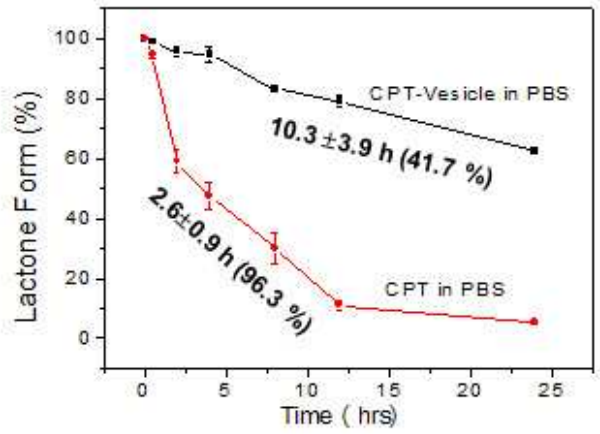


**Figure SF28.** *HPLC traces of CPT loaded vesicles incubated in PBS pH 7.4 at different time intervals (a) and Percentage of lactone form of free CPT and CPT in vesicle.*

Note: (a) HPLC traces of CPT encapsulated in vesicles indicated that the polymer scaffold retain the active lactone form. (b) Encapsulation of CPT protects 60% of active lactone form.

| Parameters | CPT in PBS | CPT-Vesicle in PBS |
|---|---|---|
| **Time** | **2.6± 0.9** | **10.3 ± 3.9** |
| **Amplitude** | **96.3 ± 11.9** | **41.7 ± 5.6** |
| **Y- intercept** | **6.1 ± 7.2** | **59.4 ± 6.2** |
| **$R^2$** | **0.96** | **0.97** |

**Table ST3.** *First order exponential hydrolysis data of CPT*

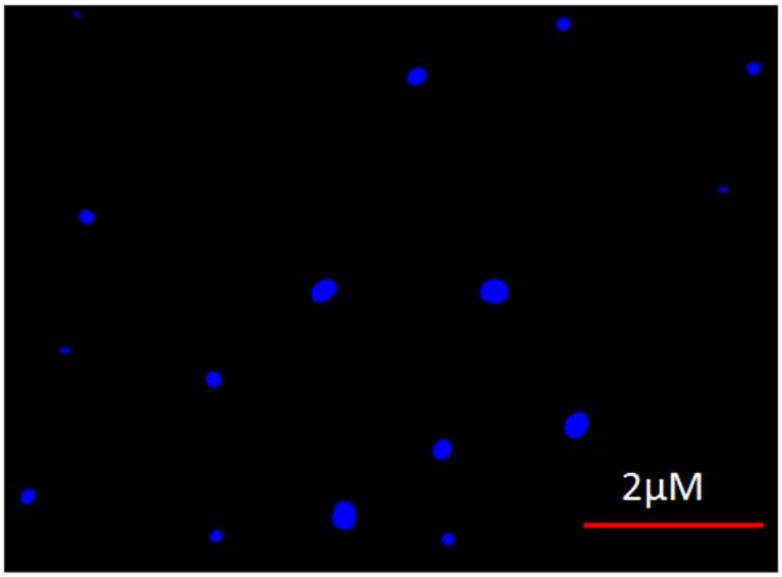


**Figure SF29.** *Fluorescent micrograph of CPT encapsulated DEX-PDP.*

Note: The aggregate appeared as blue colored spherical particles and no breakage or pores are noticed. This confirmed that the drug is very well loaded in the vesicles and their distribution was almost uniform throughout the entire polymer matrix.

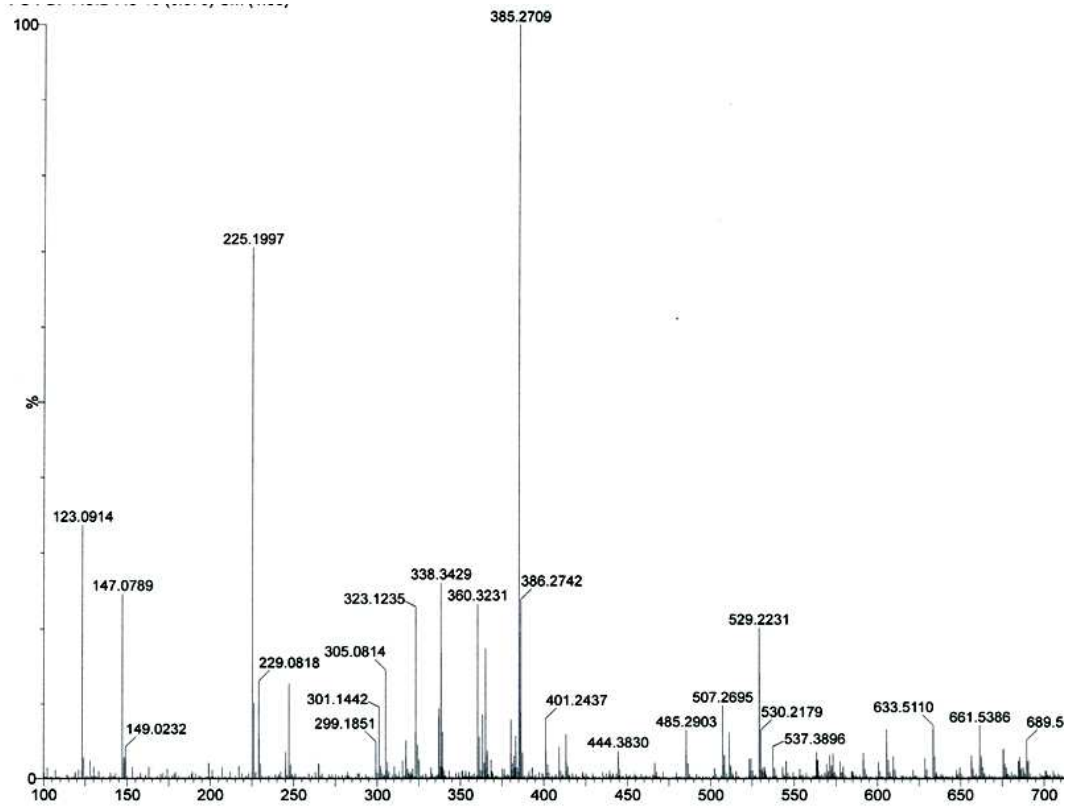


**Figure SF30:** HR-MS spectrum of PDP-acid cleaved form DEX-PDP using esterase enzyme

Note: Base peak is observed at 385.2709 is corresponding to PDP-acid $+Na^+$

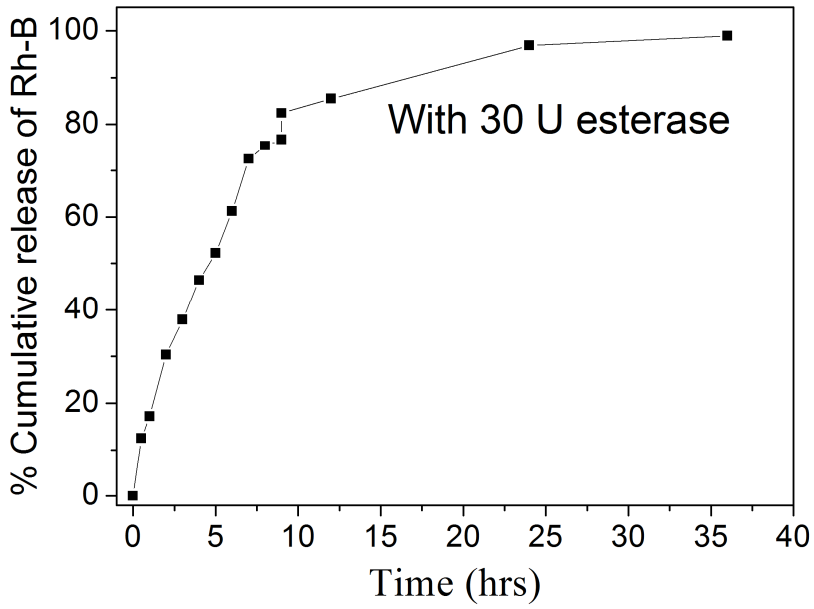


**Figure SF31.** Cumulative release of Rh-B in the presence of 30 U esterase

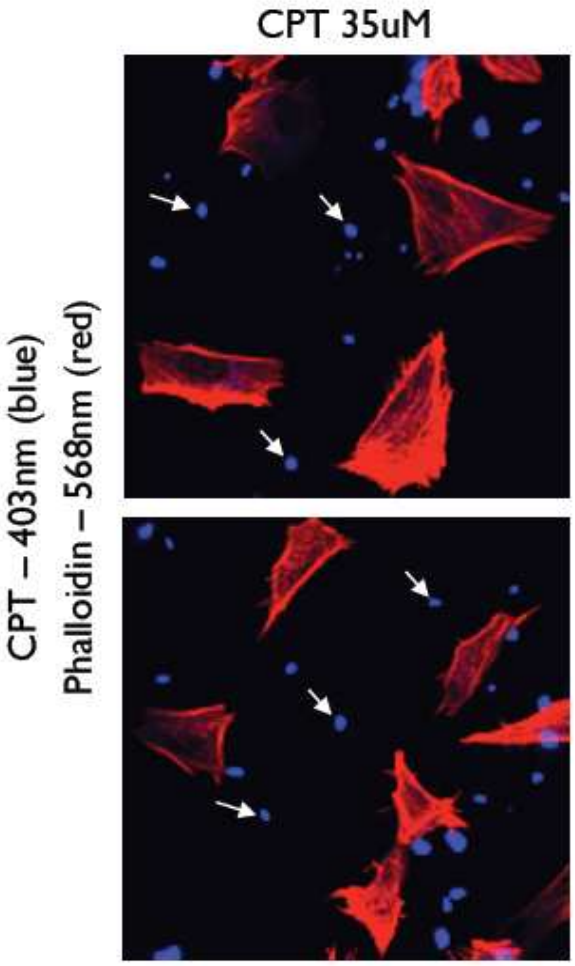


**Figure SF32.** Aggregate formation of CPT at 35uM concentration.

Note: Aggregates are stuck to the cover slip where cells are plated and their bright blue fluorescence further confirms the detection of CPT by the 403nm laser in the Confocal microscope.

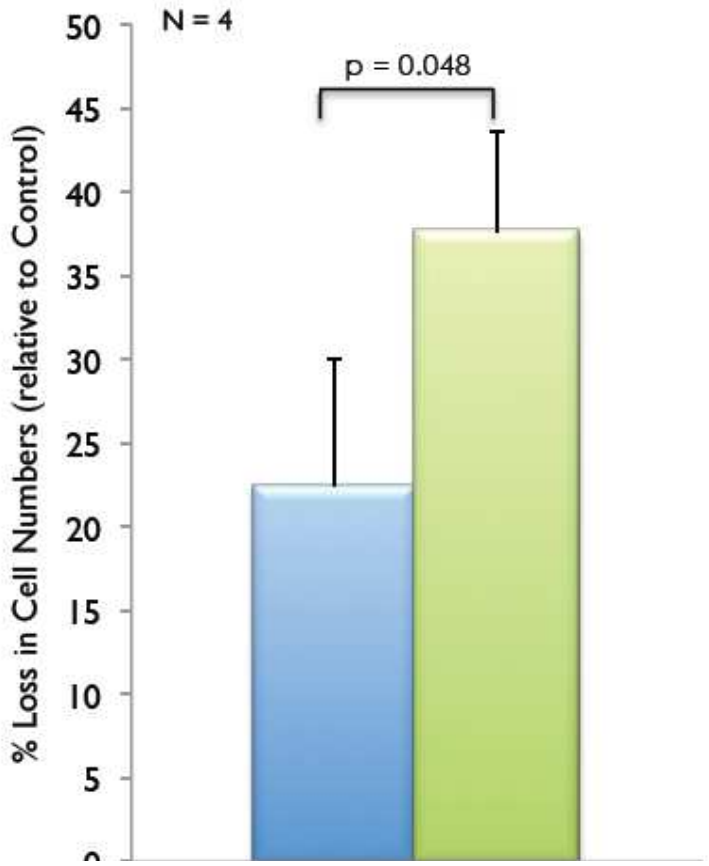


**Figure SF33.** Effect of DEX-PDP-CPT and CPT on cell viability detected by crystal violet labeling.

Note: The percentage loss in cell numbers is relative to the untreated control cells. Loss in cell numbers in larger wells of a 6 well plate could be mediated by cell death following drug treatment and also by any effects that the drug could have on adhesion of the cells to the tissue culture dishes. This effect is significantly less in the MTT assay (Figure 6b) that more specifically detects cell death and uses much lesser cells (50 times less) per well in a

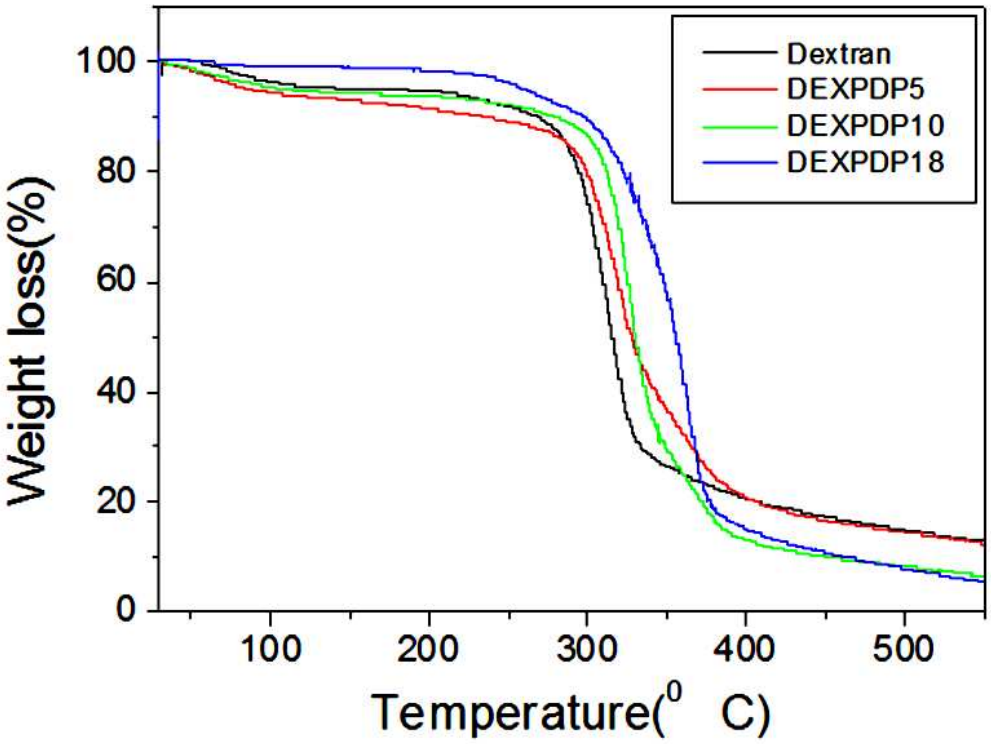


**Figure SF34.** Thermogravimetric analysis of dextran and PDP modified dextran

Note: Thermogravimetric analysis shows that DEX-PDP derivatives were stable upto 300°C, with an incremental change in the decomposition temperature as compared to dextran.

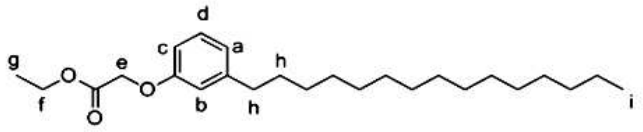


$^{1}$H NMR

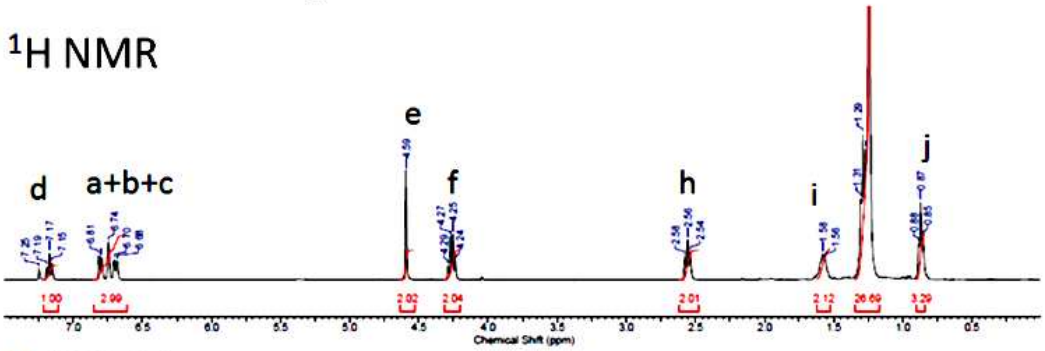


$^{13}$C NMR

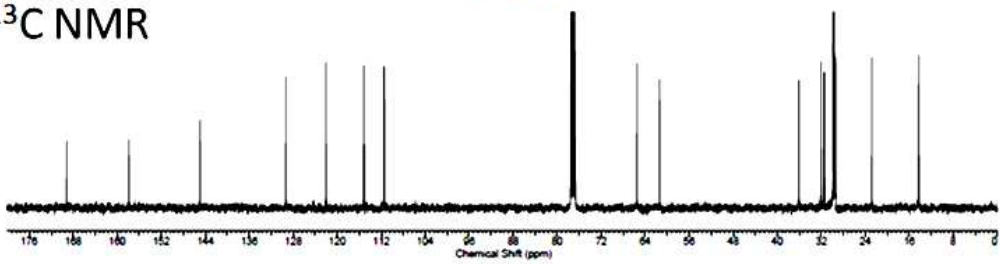


MALDI-TOF-TOF

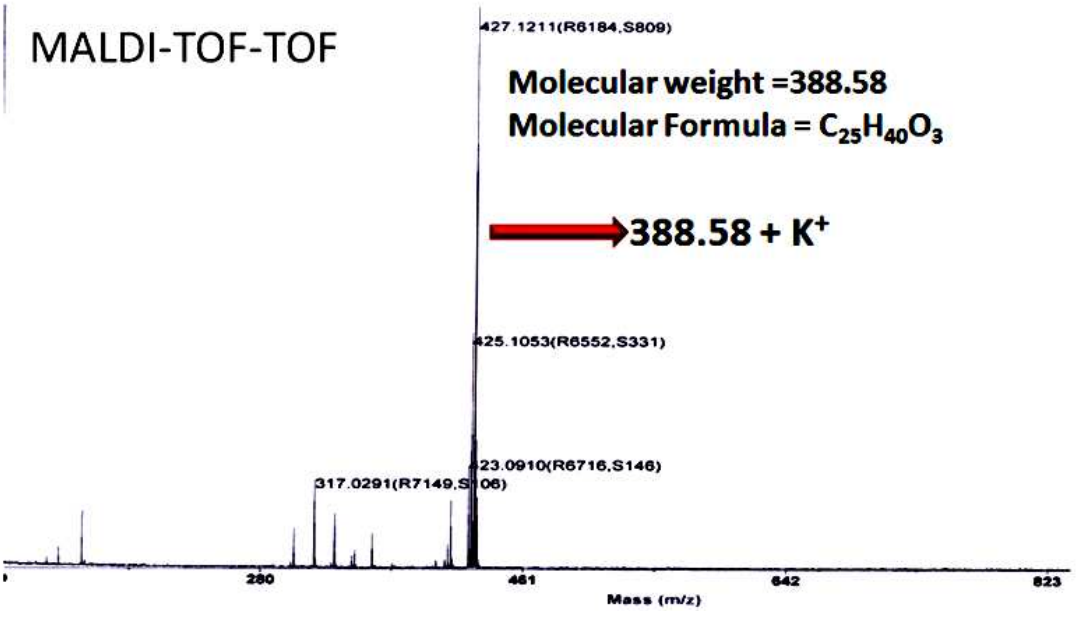

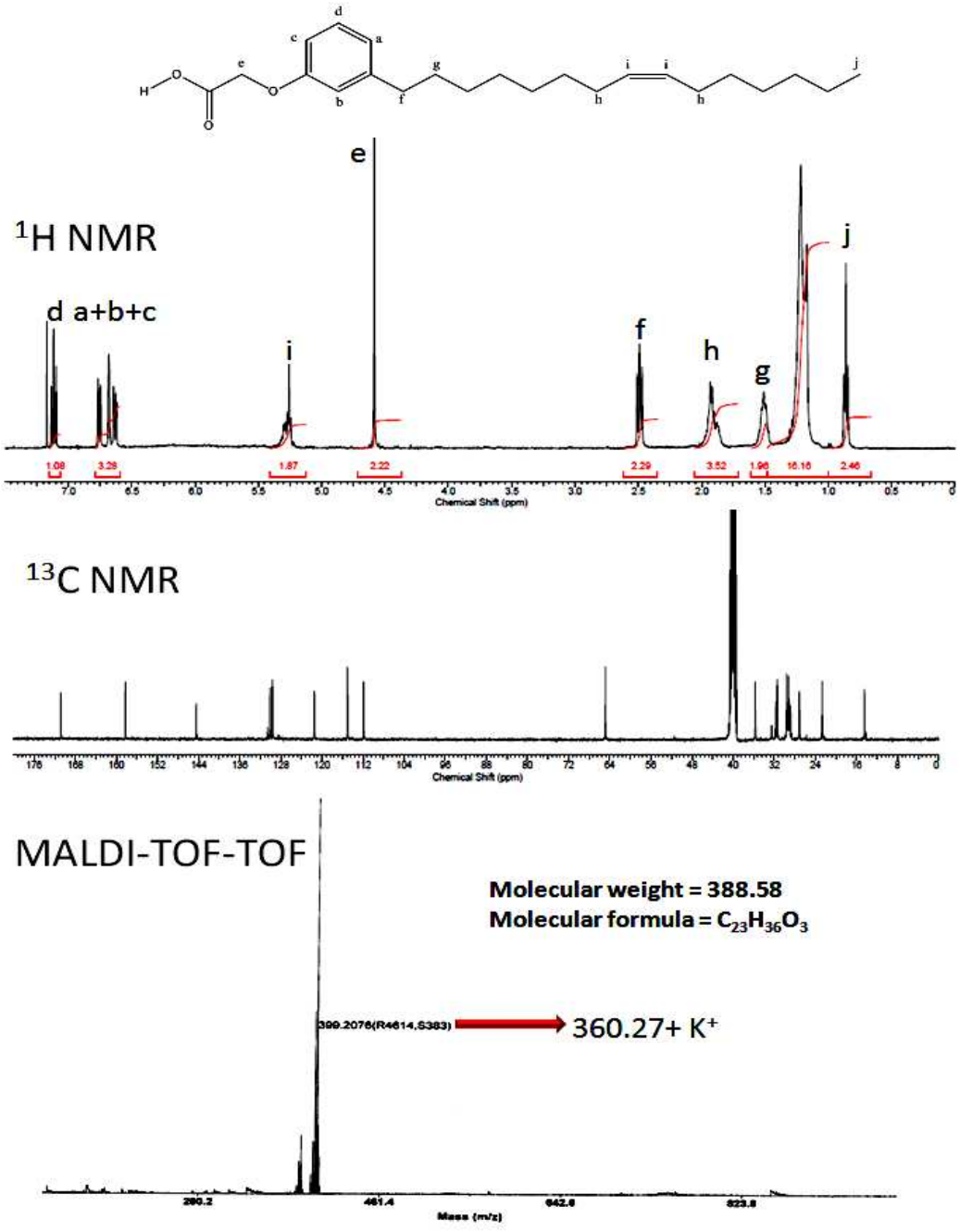
d
c
a
e
g
i
i
j
H
O
O
O
b
f
h
h
e
$^{1}$H NMR
d a+b+c
i
f
h
g
j
1.08
3.28
1.87
2.22
2.29
3.52
1.96
16.16
2.46
7.0
6.5
6.0
5.5
5.0
4.5
4.0
3.5
3.0
2.5
2.0
1.5
1.0
0.5
0
Chemical Shift (ppm)
$^{13}$C NMR
176
168
160
152
144
136
128
120
112
104
96
88
80
72
64
56
48
40
32
24
16
8
0
Chemical Shift (ppm)
MALDI-TOF-TOF
Molecular weight = 388.58
Molecular formula = $C_{23}H_{36}O_3$
389.2076(R4614.5383)
360.27+ $K^+$
280.2
461.4
642.6
823.8
Mass (m/z)

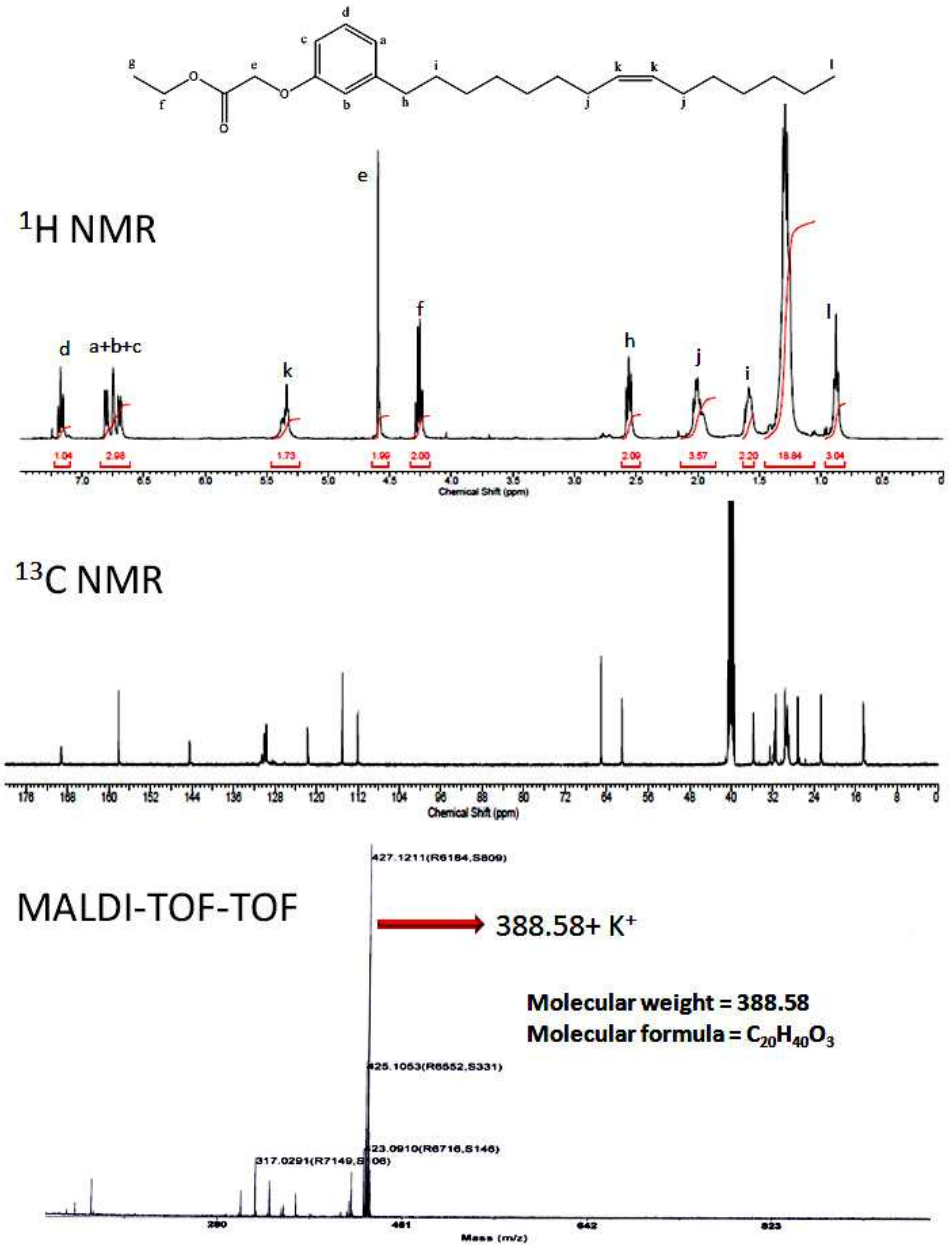
$^{1}$H NMR
$^{13}$C NMR
MALDI-TOF-TOF
388.58+ K+
Molecular weight = 388.58
Molecular formula = C20H40O3
427.1211(R6184,S809)
425.1053(R6552,S331)
423.0910(R6716,S146)
317.0291(R7149,S108)
Chemical Shift (ppm)
Mass (m/z)

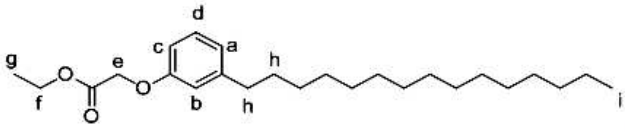


$^{1}$H NMR

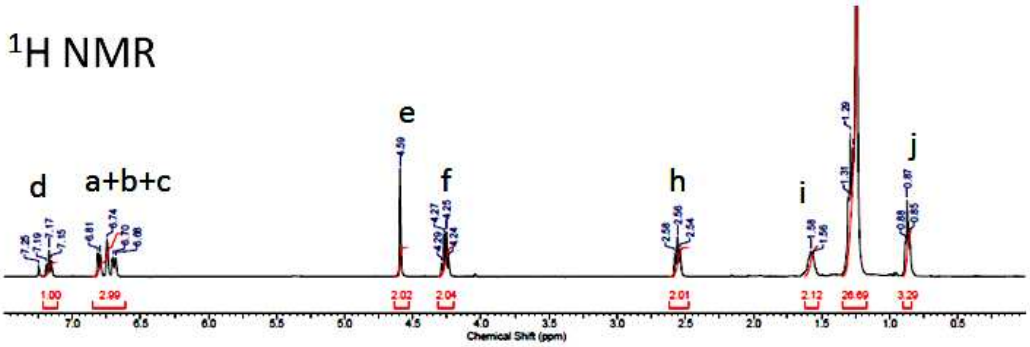


$^{13}$C NMR

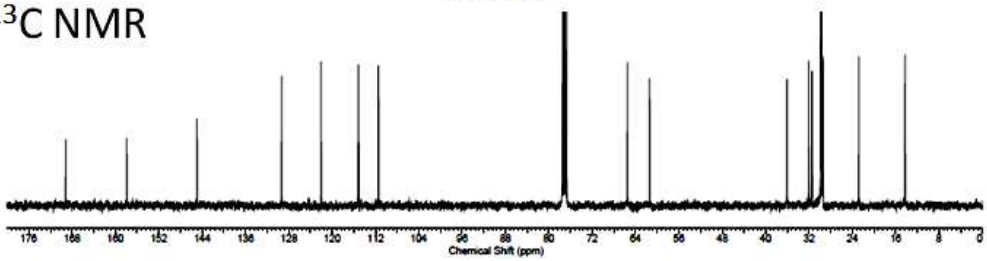


MALDI-TOF-TOF

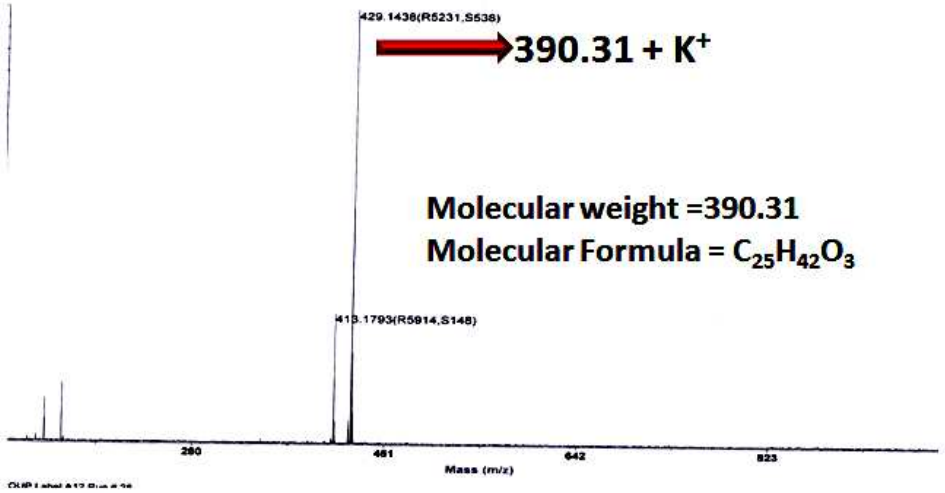

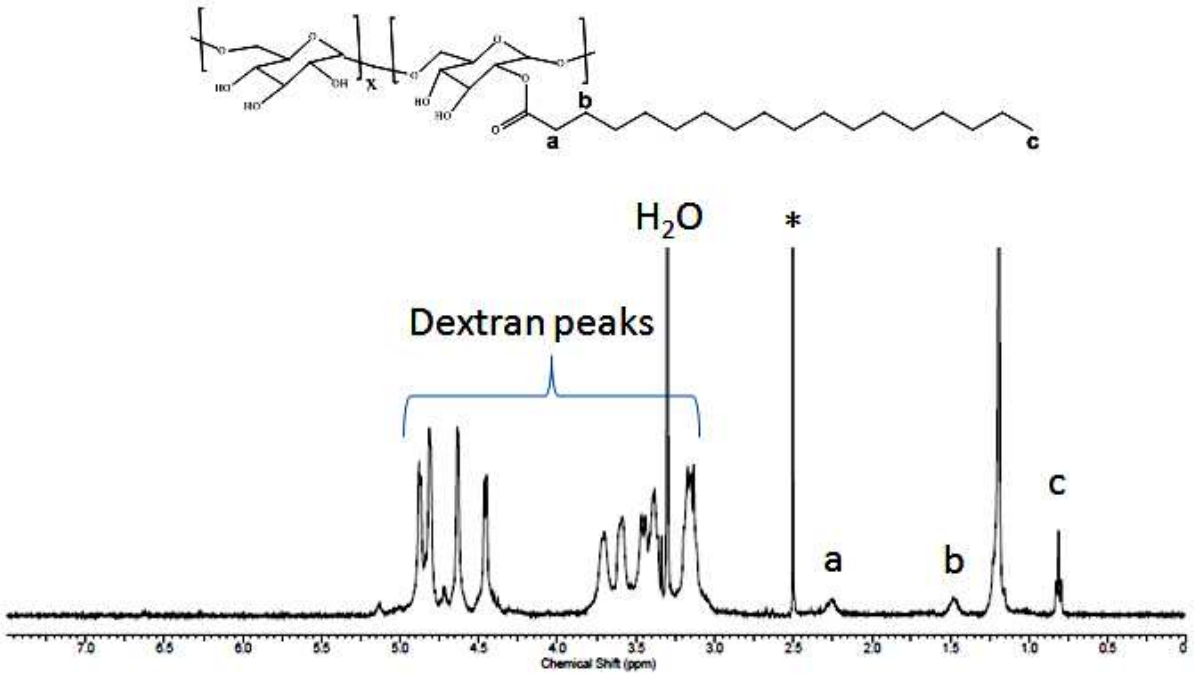


$^{1}$H NMR spectrum of DEX-SA